Study on Semiconductor Lasers of Circular Structures Fabricated by EB Lithography

Ashim Kumar Saha (D3)

Supervisor: Prof. Toshiaki Suhara

Doctoral Thesis Defense

Quantum Engineering Design Course
Graduate School of Engineering, Osaka University

Background

➢ Semiconductor lasers of circular geometry have many potential advantages for applications including laser display, printers, optical interconnects, sensing and THz wave generation.

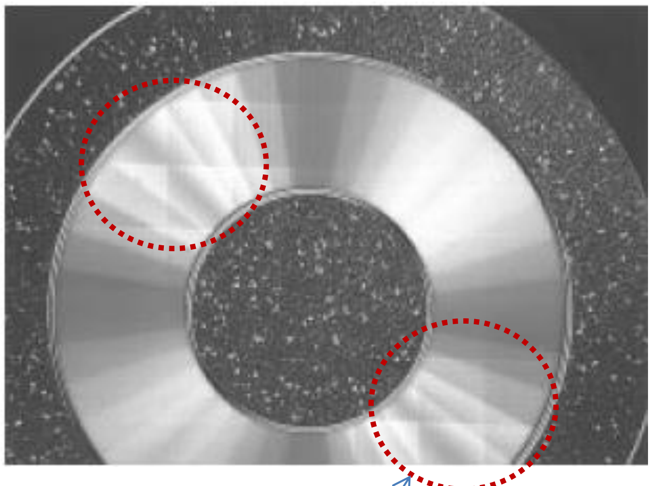

gratings are "stitched" together with sectors [1]

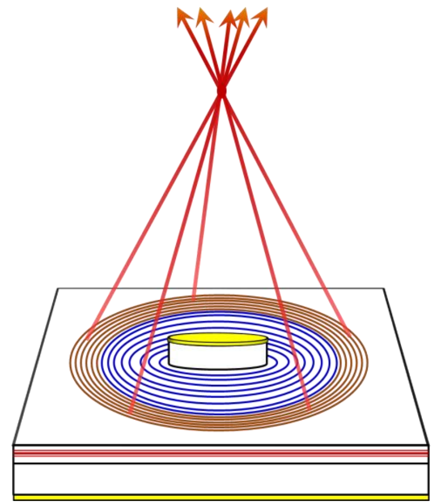

- 2D array formation
- beam shaping function

Circular-Grating-Coupled Surface Emitting Lasers

[1] S. Kristjansson, M. Li, N. Eriksson, M. Hagberg, K.-J. Killius, and A. Larsson, *IEEE Photon. Technol. Lett.*, vol. 9, p. 416, 1997.

1. Introduction

Background

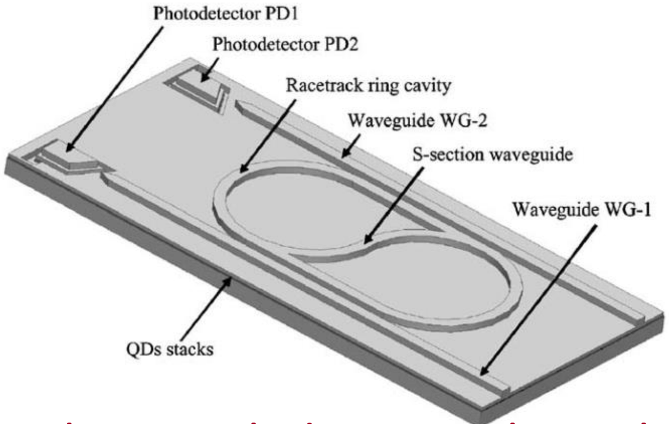

Ring laser with directional coupler [2]

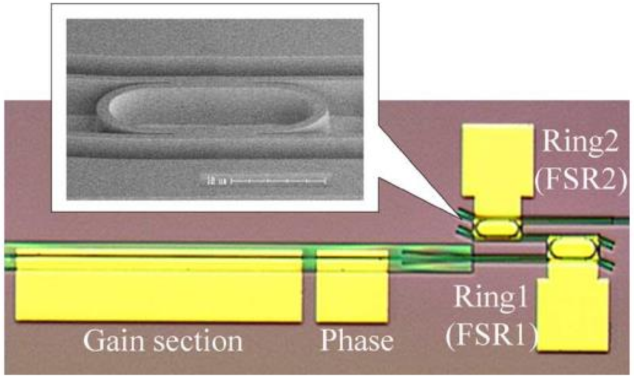

Laser with MMI coupler [3]

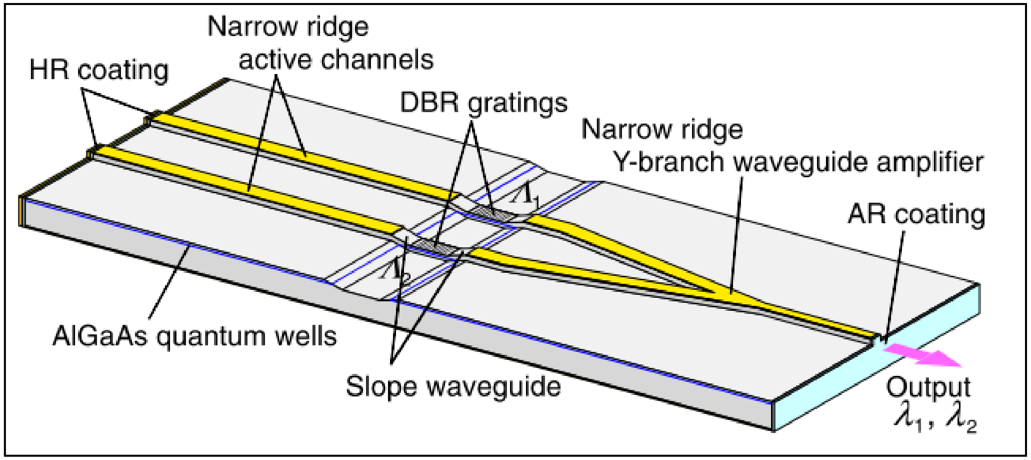

Monolithic dual-wavelength diode lasers [4]

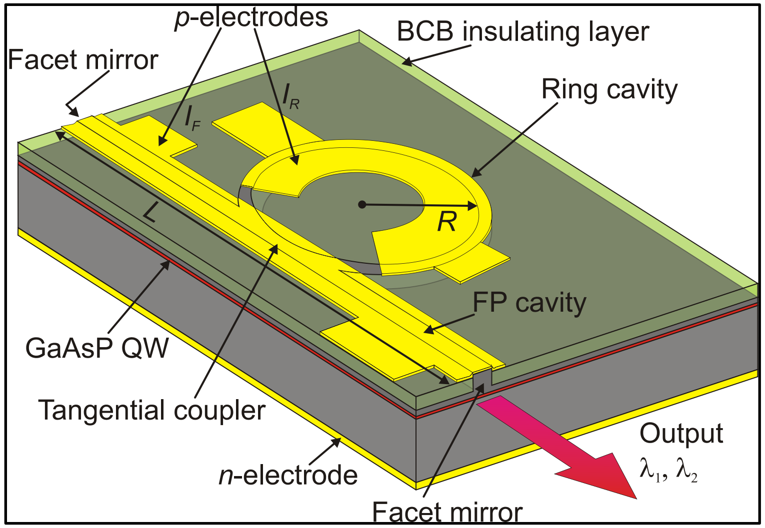

Application for THz wave generation

[2] M. Osiński, H. Cao, C. Liu, and P. G. Eliseev, J. Cryst. Growth, vol. 288, no. 1, pp. 144–147, Feb. 2006.
[3] S. Matsuo and T. Segawa, IEEE J. Sel. Top. Quantum Electron., vol. 15, no. 3, pp. 545–554, 2009.
[4] M. Uemukai, H. Ishida, A. Ito, T. Suhara, H. Kitajima, A. Watanabe, and H. Kan, Jpn. J. Appl. Phys., 51, 020205 (2012).

Technological issues

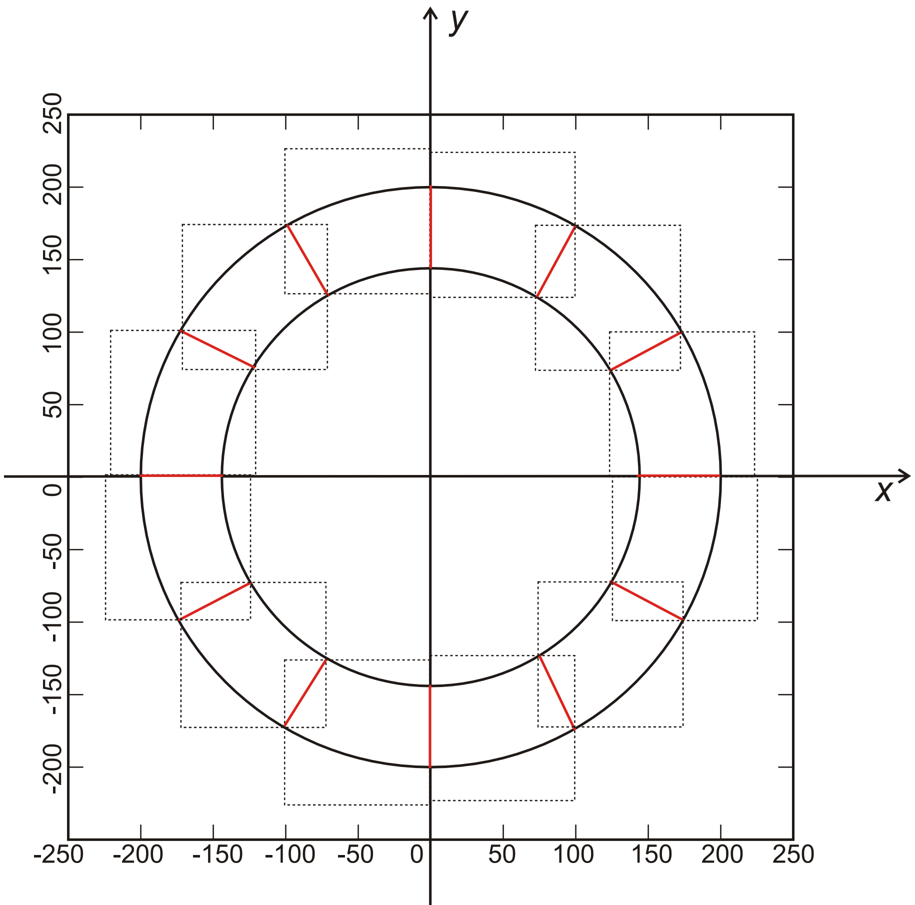

field size 80μm × 80μm

Conventional EB writing of circular grating

Continuous circular scanning of e-beam

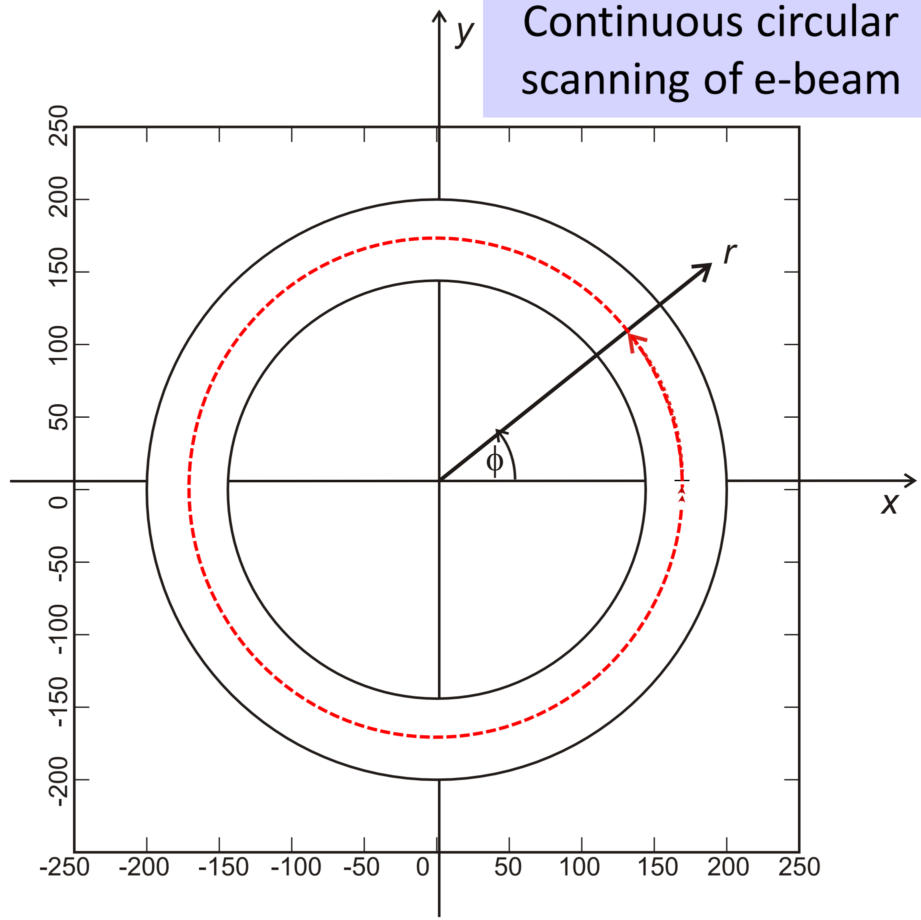

field size 500μm × 500μm

Circular gratings of fine groove (<100 nm) over large area (~500 μm)

EB writing of circular grating by ELS3700S

Aim of My Work

- My research subjects are the study of integrated semiconductor lasers having circular geometry, aiming to the application for beam shaping function and THz wave generation .

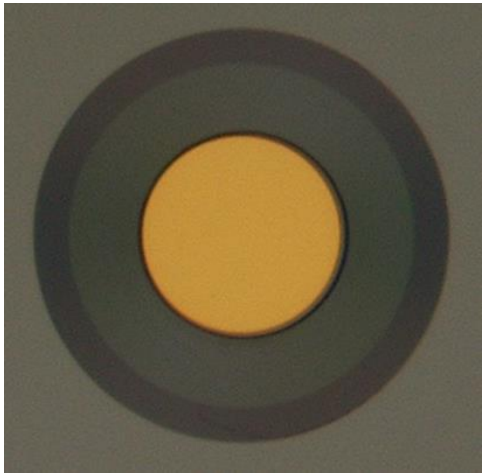

CGCSEL with focusing function

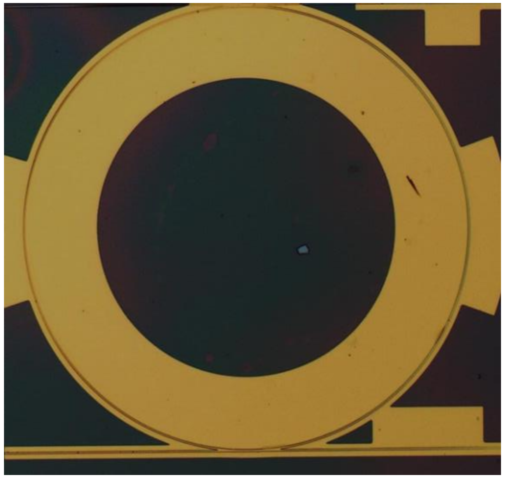

Single mode RFP Laser

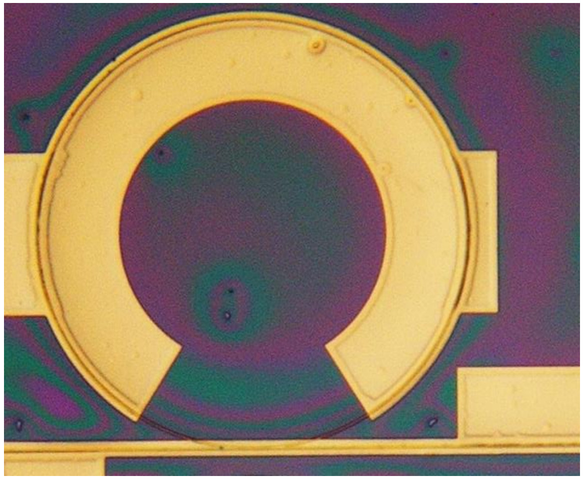

Two-wavelength RFP Laser

- In my thesis work, I demonstrate the design, fabrication and experimental results of those lasers.

CGCSEL with Focusing Function

- InGaAs based CGCSEL which emits light at 980 nm wavelength was designed, fabricated and evaluated.

I designed the DBR and GC by **Coupled Mode Theory**

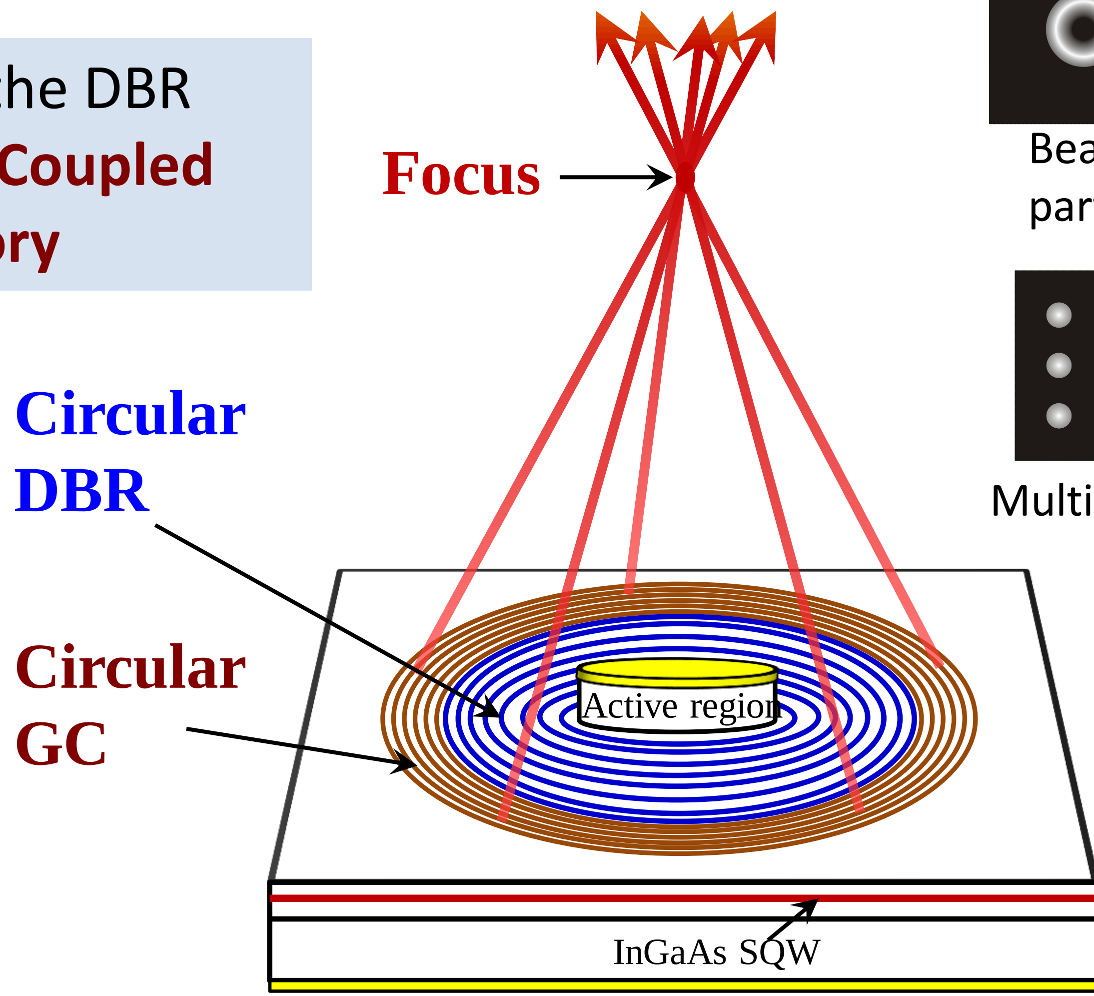

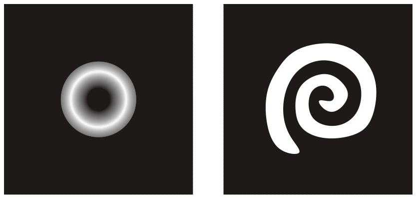

Beam shaping for particle trapping

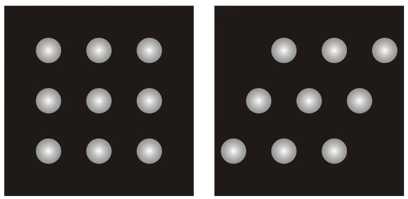

Multiple spot formation

Design of Circular DBR

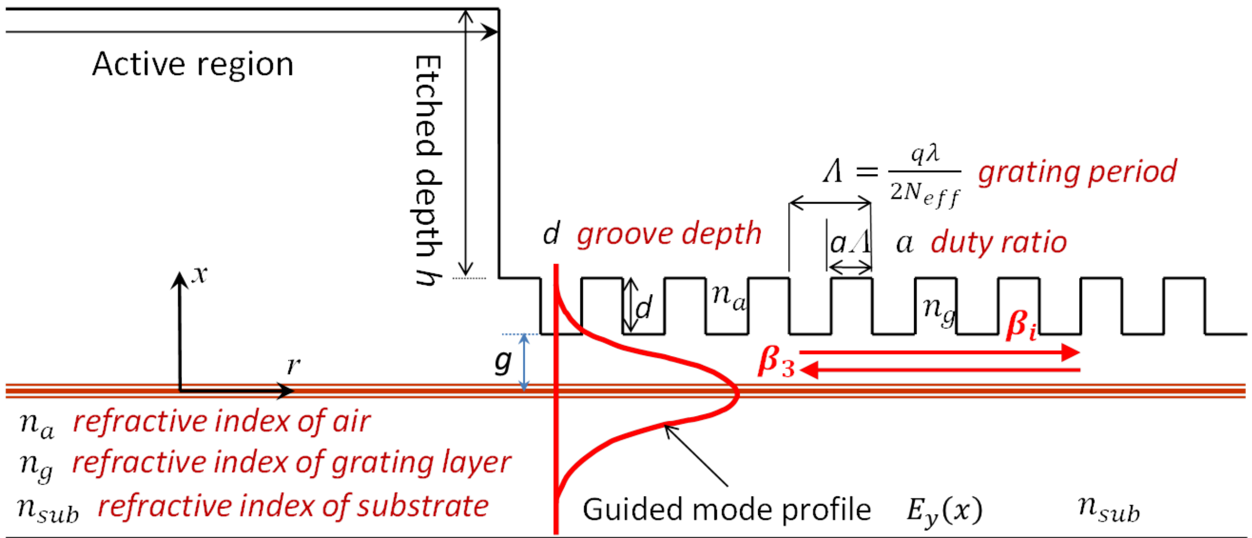

3rd order coupling coefficient κ_3 was calculated by:

$$\kappa_3 = \frac{k_0}{2N_{eff}} \Delta\epsilon_3 \frac{\int_g^{g+d} |\boldsymbol{E_y}(x)|^2 dx}{\int_{-\infty}^{\infty} |\boldsymbol{E_y}(x)|^2 dx}$$

$$\Delta\epsilon_3 = (n_g^2 - n_a^2) \frac{\sin(3a\pi)}{3\pi}$$

$\Delta\varepsilon_3$ is the amplitude of 3rd order Fourier component.

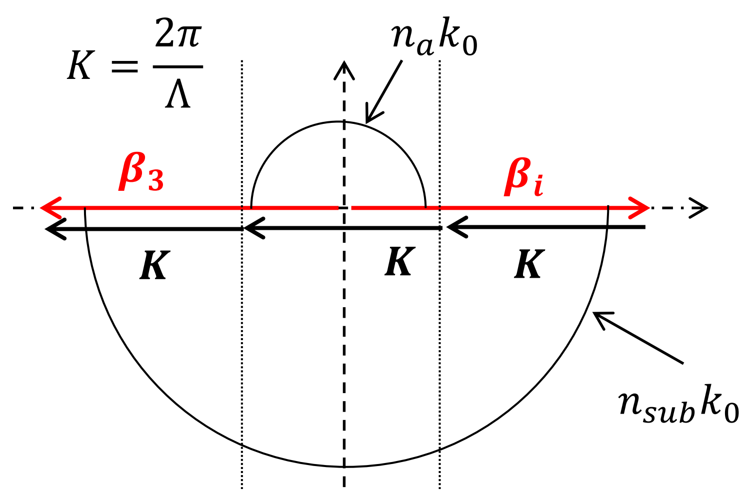

Wave vector diagram of 3rd order DBR

Design of Circular GC with Focusing Function

Applying phase matching condition, period $\Lambda(r)$ of the 1st order grating coupler with focusing function can be written as:

$$N_{eff}k_0 + n_a k_0 \sin\theta(r) = K(r)$$

$$N_{eff}\frac{2\pi}{\lambda} + \frac{2\pi}{\lambda}\sin\theta(r) = \frac{2\pi}{\Lambda(r)}$$

$$\Lambda(r) = \frac{\lambda}{\frac{r}{\sqrt{r^2+f^2}} + N_{eff}}$$

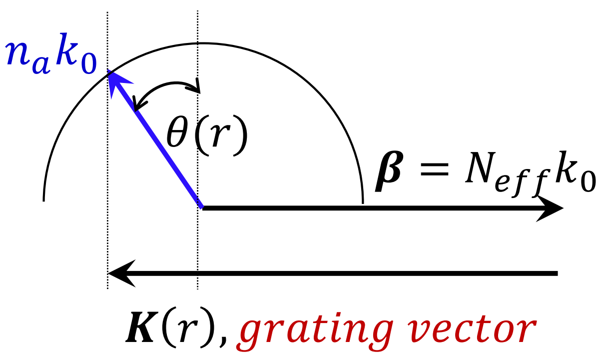

Wave vector diagram of 1st order grating coupler

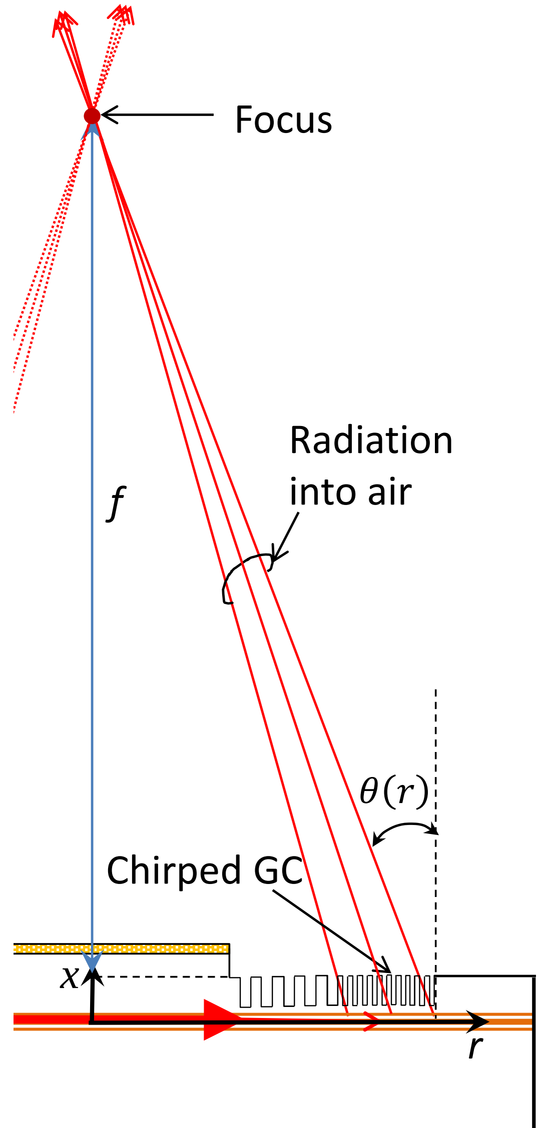

Calculation results for DBR and GC

based on the **Coupled Mode Theory** and **Transfer Matrix Method**

$P_{air} = \alpha_{air}/(\alpha_{air}+\alpha_{sub}+\alpha_{abs})$

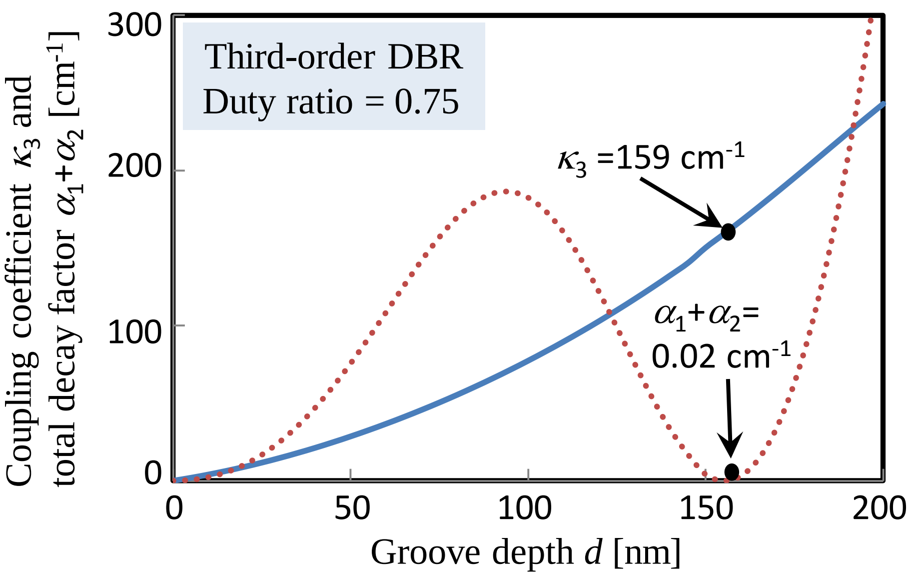

Dependence of third-order coupling coefficient κ_3 and total radiation decay factor $\alpha_1+\alpha_2$ on the DBR groove depth.

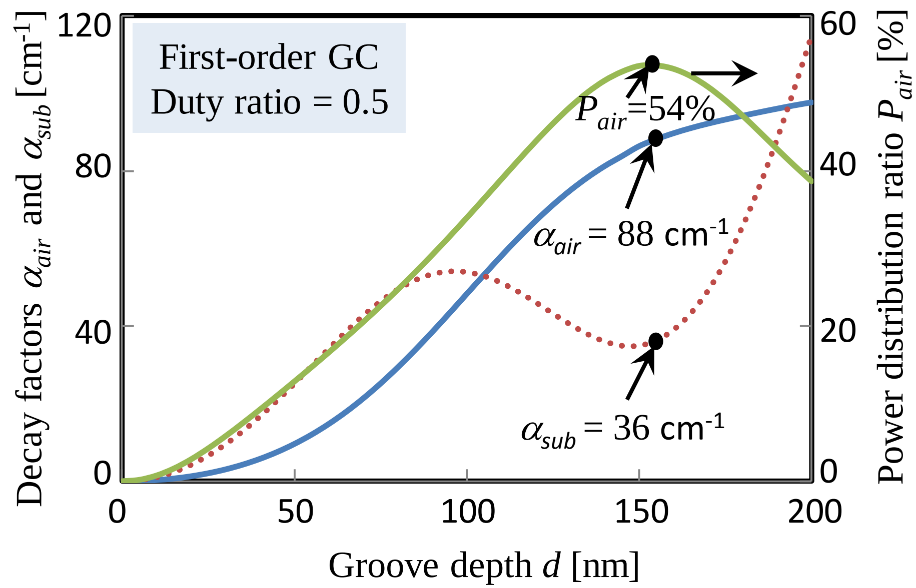

Dependence of α_{air}, α_{sub} and P_{air} on the GC groove depth calculated by assuming α_{abs} = 40 cm^{-1} .

Fabrication of CGCSEL

➢ Formation of circular active region

➢ I have written a computer program to control the electron beam writing system with circular scanning mode.

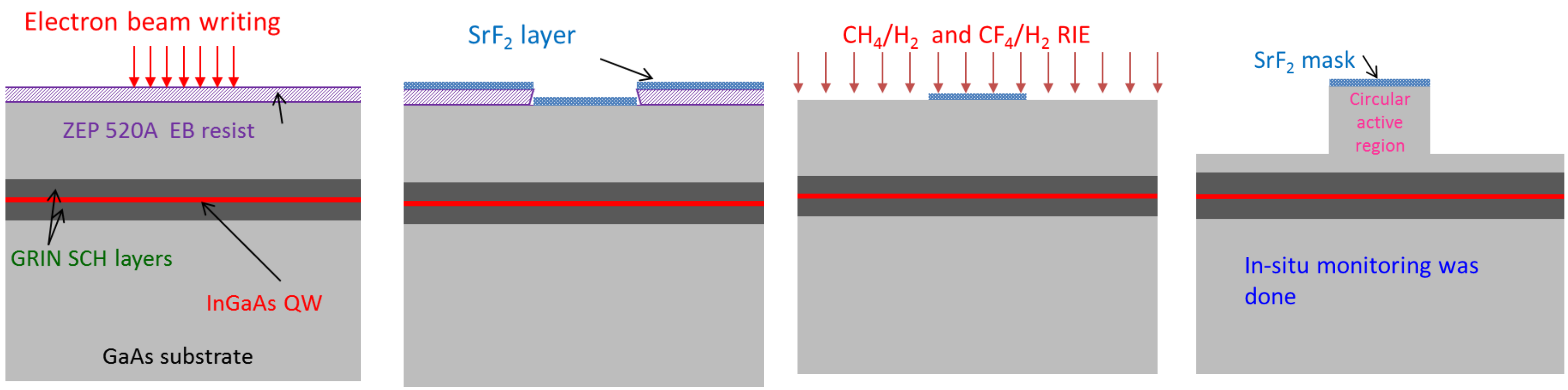

Fabrication of CGCSEL

➢ DBR and grating coupler fabrication

Circular DBR and GC were fabricated by electron beam lithography employing the smooth circular scanning and two step RIE.

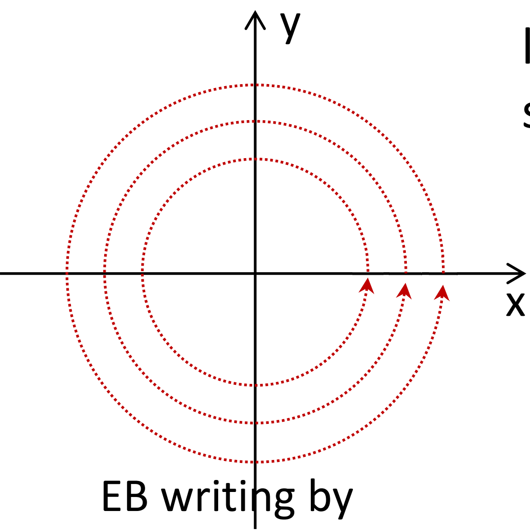

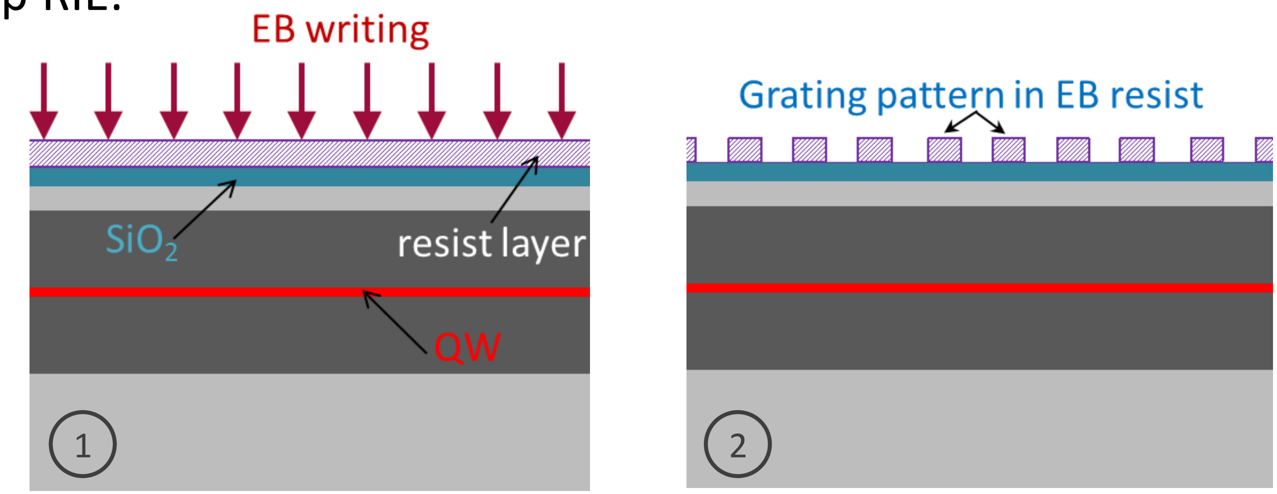

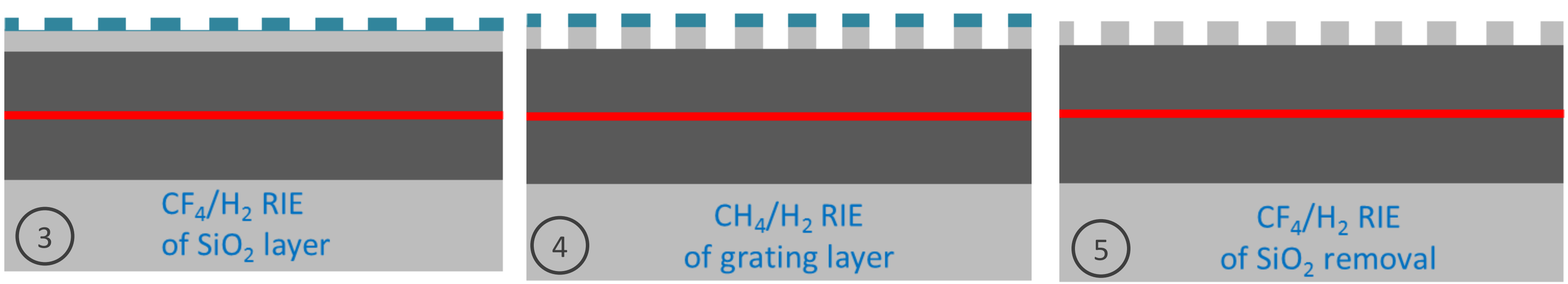

➢ p-side and n-side electrode formation

Fabricated CGCSEL

- DBR and GC gratings of almost uniform duty ratios were fabricated.

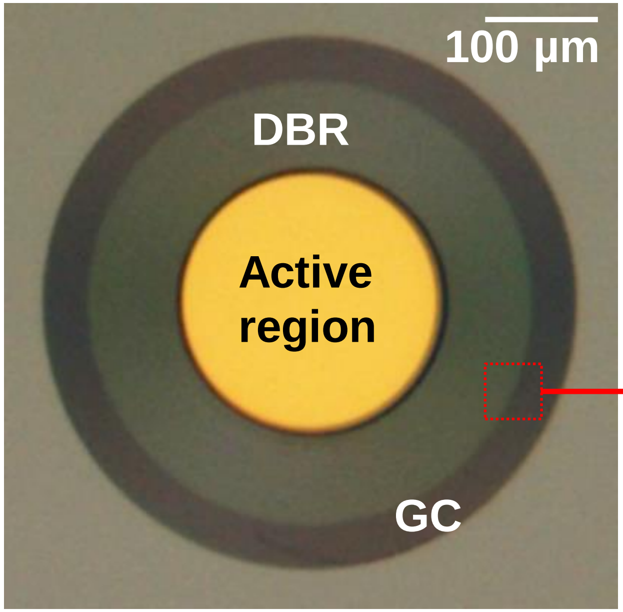

Optical microscopic image of the fabricated CGCSEL.

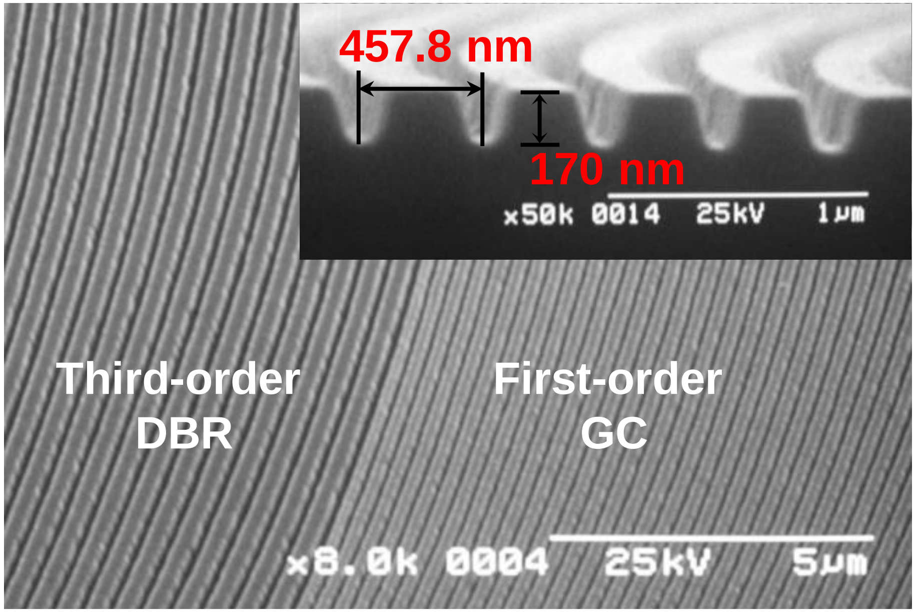

SEM images of the DBR and the chirped GC. Inset is the cross sectional view of the DBR.

Lasing Characteristic of the CGCSEL

- Single mode lasing was accomplished.

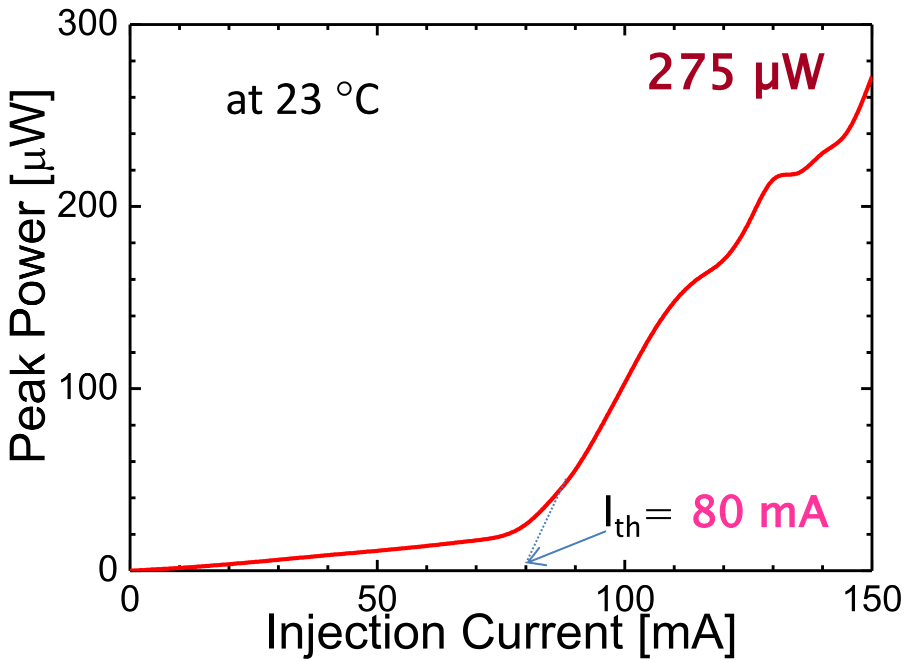

P-I characteristic of the CGCSEL

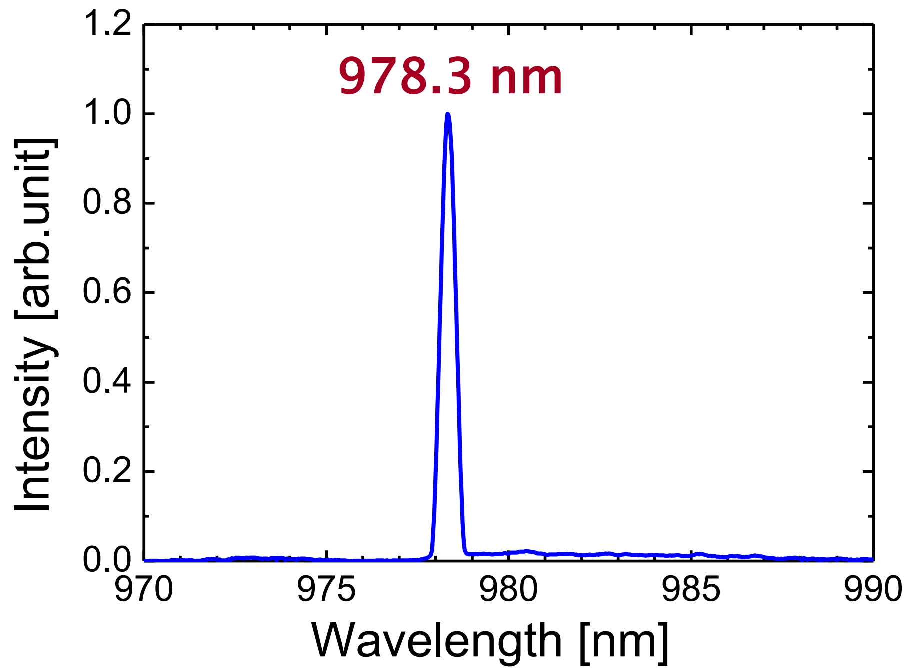

lasing spectrum measured at 115mA

Focusing Function

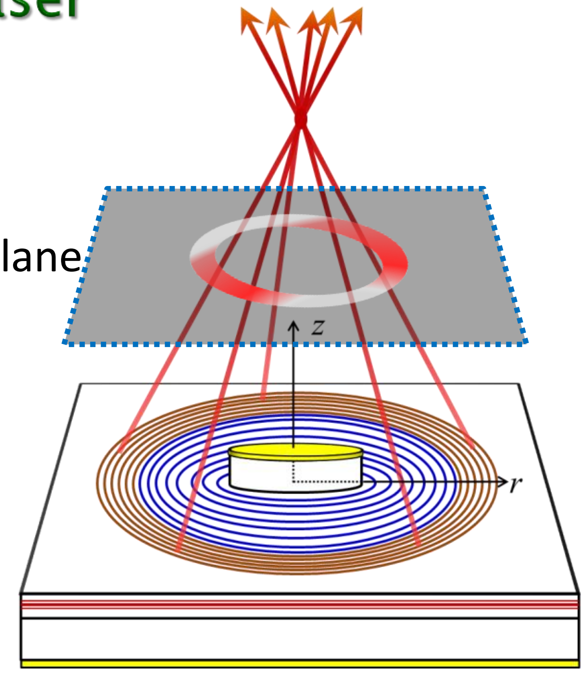

Intensity variation comparable to a $\cos^2\phi$ dependence corresponding to lasing in $TE_{\phi 1}$ mode.

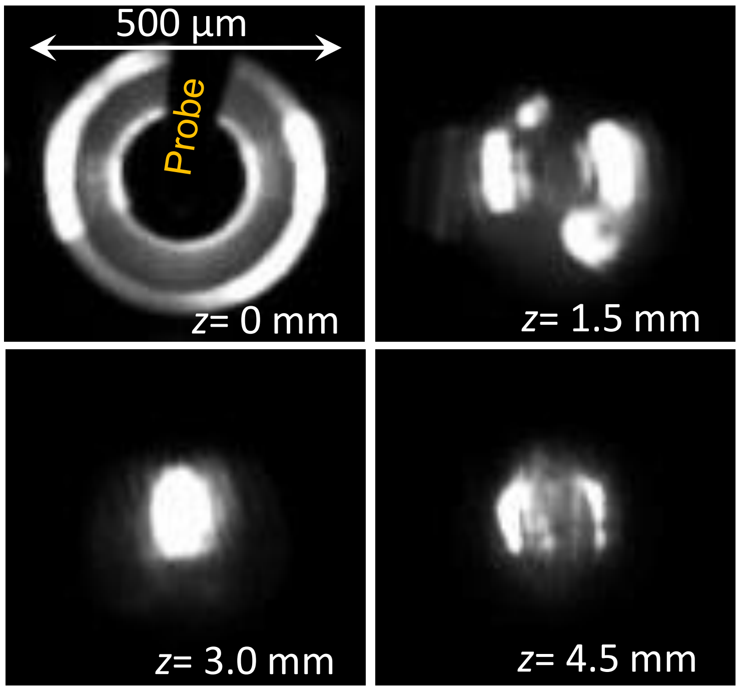

Emission patterns at different distances *z* from the laser surface at an injection current of 140 mA

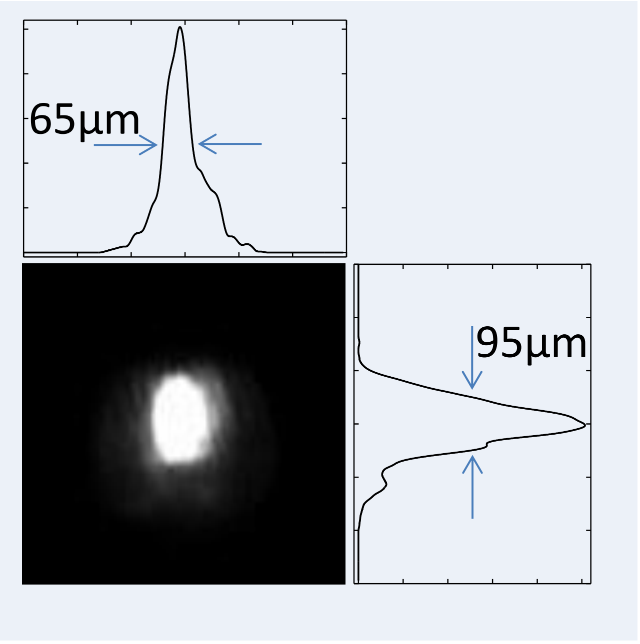

3. Theoretical Analysis and Design of Ring/Fabry-Perot Composite Cavity Lasers

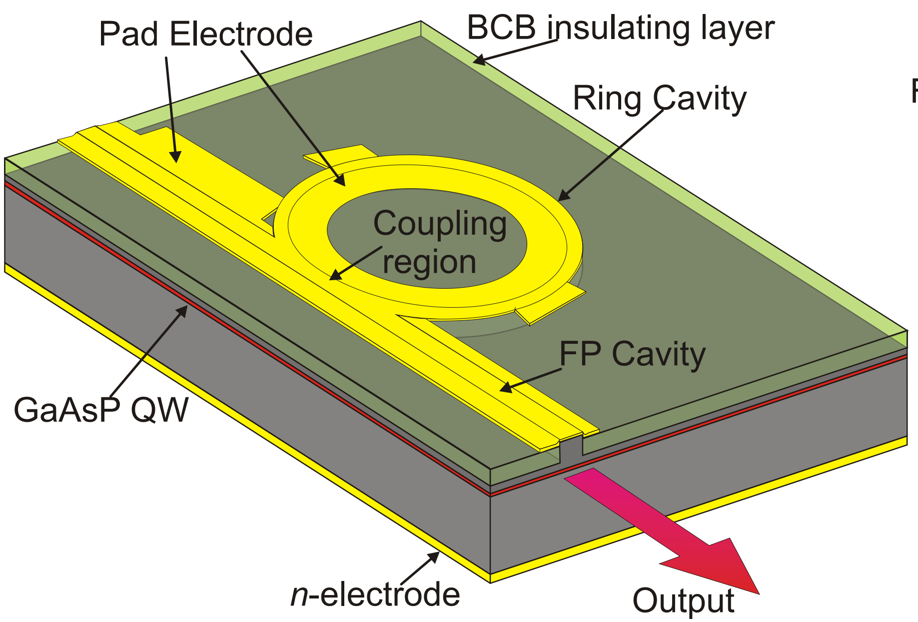

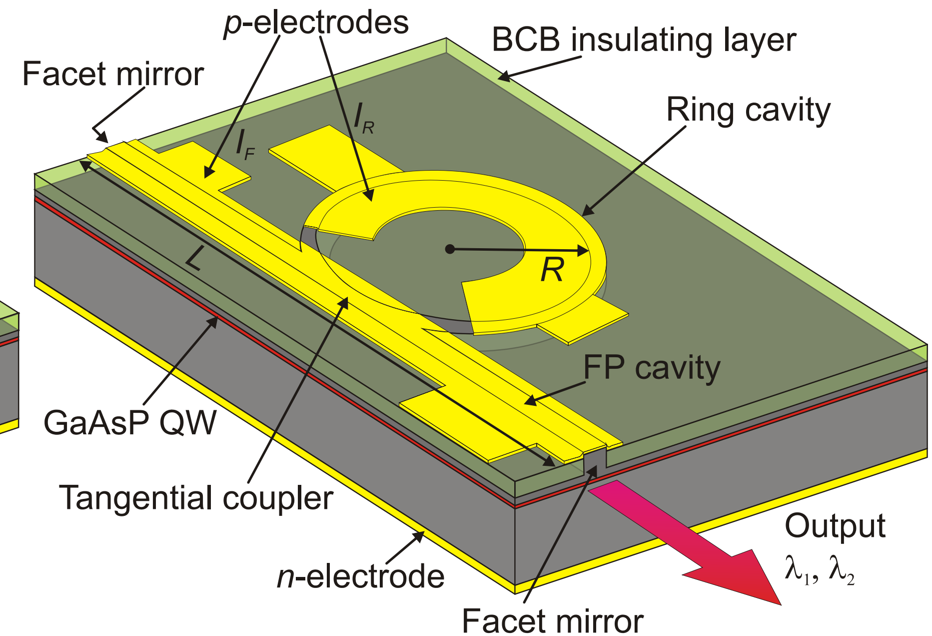

- Simple fabrication because it does not require narrow gaps or deep etching
- Useful for of THz wave generation

Composite Resonator

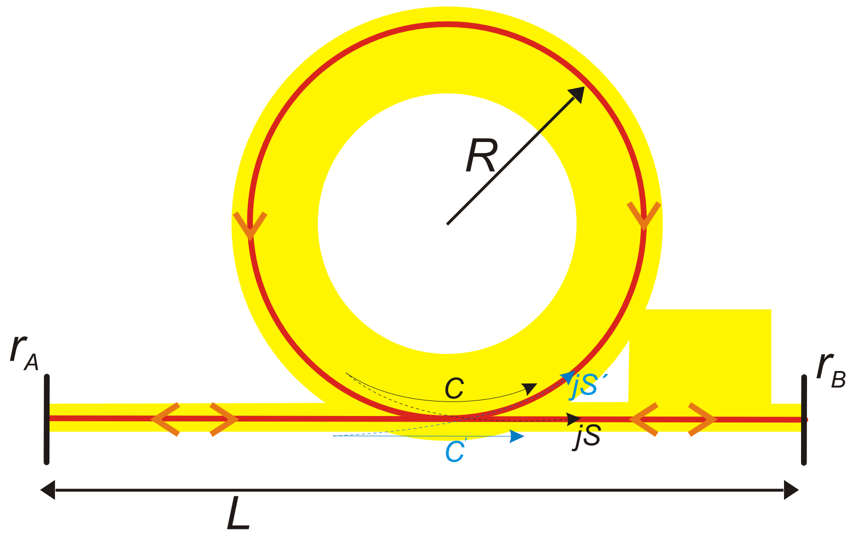

Ring cavity: $f_{Rm} = \frac{c}{2\pi R n_{Re}} m, \quad \Delta f_R = \frac{c}{2\pi R n_{Reg}}$

FP cavity: $f_{Fm'} = \frac{c}{2L n_{Fe}} m', \quad \Delta f_F = \frac{c}{2L n_{Feg}}$

n_{Re} (n_{Reg}), n_{Fe} (n_{Feg}): effective (effective group) refractive indices

m, m': mode numbers for the ring and FP cavities

Lasing condition

Composite cavity ring/FP laser with **active** ring and FP section

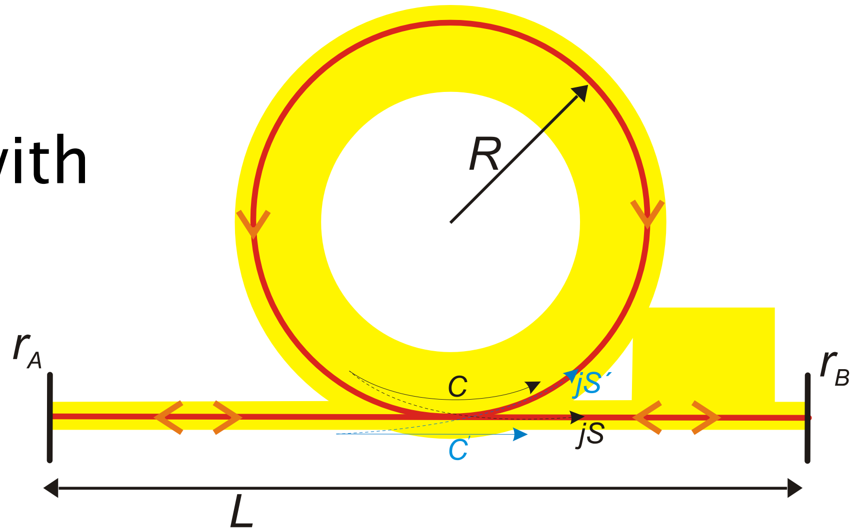

Complex round trip gain =1

$$r_A r_B \left(\frac{C' - \eta e^{-j\tilde{\beta} 2\pi R}}{1 - C e^{-j\tilde{\beta} 2\pi R}} \right)^2 e^{-j2\tilde{\beta} L} = 1$$

$G_R = e^{g\pi R}$
$G_L = e^{gL}$

$\tilde{\beta} = \beta + j\frac{g}{2}$: complex propagation constant

g : intensity gain factor

$\eta = CC' + SS'$

$$r_A r_B \left(\frac{-C' + \eta G_R e^{-j\beta 2\pi R}}{1 - C G_R e^{-j\beta 2\pi R}} \right)^2 G_L e^{-j\beta 2L} = 1 \qquad (1)$$

Lasing condition

Assuming $n_{Re} = n_{Fe} = n_e$ and
$n_{Reg} = n_{Feg} = n_{eg}$

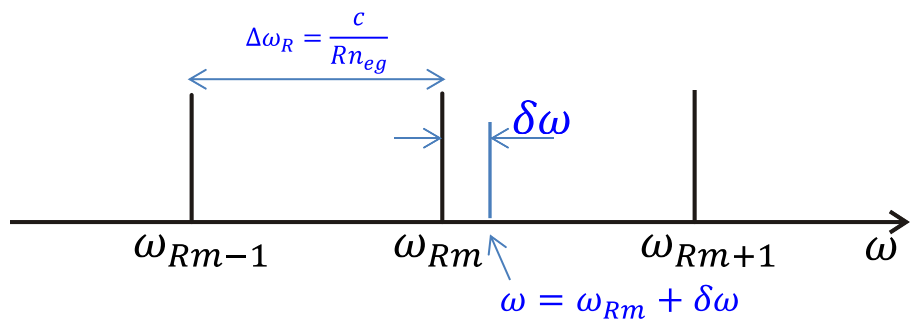

Putting $\beta = n_e \frac{\omega}{c} = \beta_{Rm} + \delta\beta = \beta_{Rm} + \frac{n_{eg}}{c}\delta\omega$ in (1)

Phase condition:

$$2\arg\left\{\frac{-C' + \eta G_R \mathrm{e}^{-j\delta\beta 2\pi R}}{1 - C G_R \mathrm{e}^{-j\delta\beta 2\pi R}}\right\} - 2(\beta_{Rm} + \delta\beta)L = -2M\pi \qquad (2)$$

M : is the composite mode number

Amplitude condition:

$$r_A r_B \frac{(\eta G_R - C')^2 + 4C'\eta G_R \sin^2(\delta\beta\pi R)}{(1 - C G_R)^2 + 4C G_R \sin^2(\delta\beta\pi R)} G_L = 1 \qquad (3)$$

Lasing condition

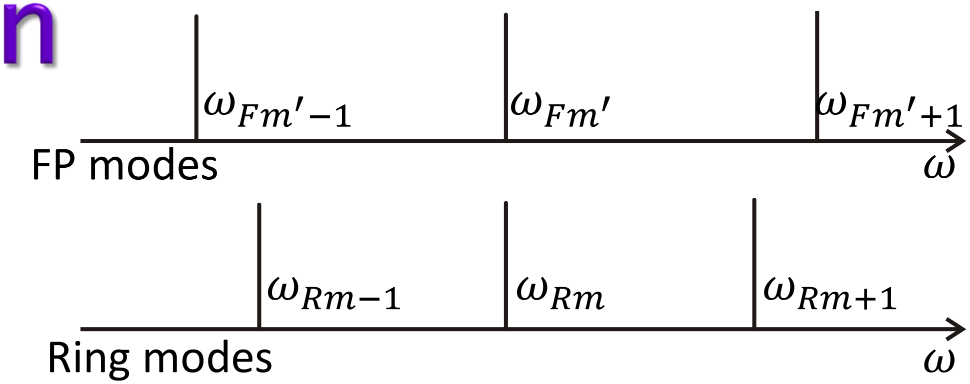

Case I: $\omega_{Rm} = \omega_{Fm'}$

Phase condition is satisfied by $\omega = \omega_{Rm} = \omega_{FPm'}$. Hence the composite cavity mode is at this frequency.

Amplitude Condition:

$$r_A r_B \left(\frac{\eta e^{g\pi R} - C'}{1 - C e^{g\pi R}} \right)^2 e^{gL} = 1$$

Composite mode can lase only if

$$G_R |C| < 1$$

$$r_A r_B |C'|^2 G_L < 1$$

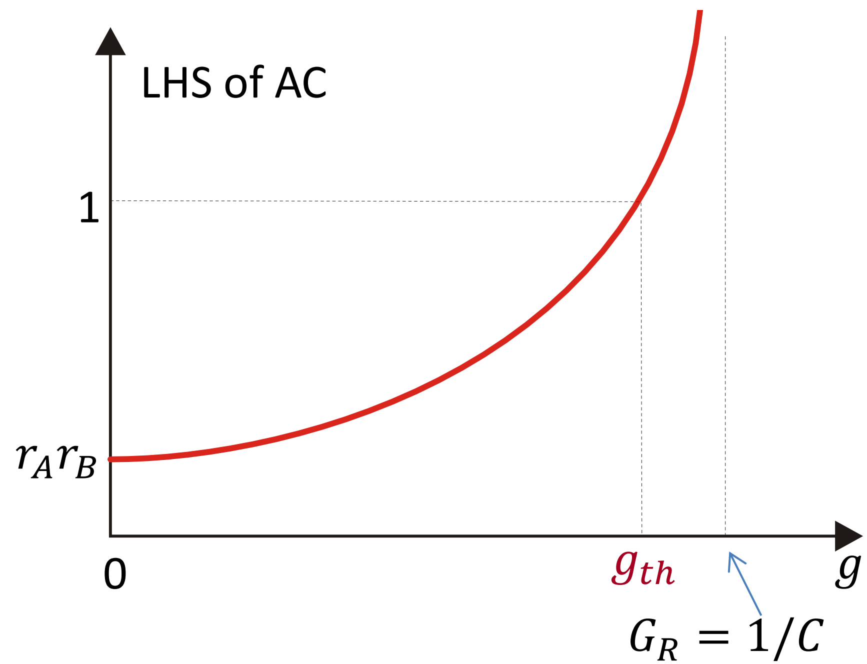

Lasing condition

Case II: $\omega_{Rm} \neq \omega_{Fm'}$

$$\Delta\omega \ll \Delta\omega_R, \Delta\omega_F$$

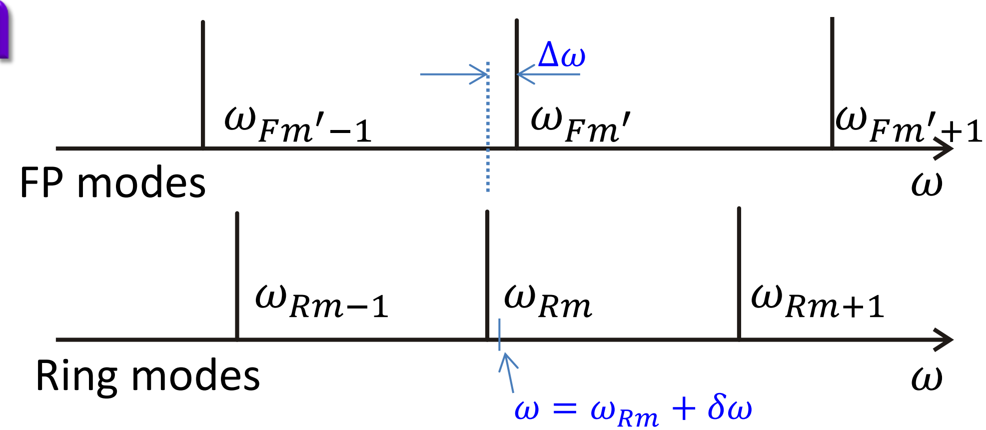

Phase condition:

$$2\arg\left\{\frac{-C' + \eta G_R e^{-j\delta\beta 2\pi R}}{1 - CG_R e^{-j\delta\beta 2\pi R}}\right\} - 2(\delta\beta - \Delta\beta)L = -2(M - m')\pi$$

For $C < G_R < \frac{1}{C}$, $|\delta\beta 2\pi R| \ll 1$ and $M = m'$, we have

$$\delta\beta = \frac{\Delta\beta}{1 + \frac{G_R S S' 2\pi R}{(\eta G_R - C')(1 - CG_R)L}}$$

Since, $0 < \frac{\delta\beta}{\Delta\beta} < 1$ hence $0 < \frac{\delta\omega}{\Delta\omega} < 1$, the composite cavity mode frequency ω is between the FP mode and ring mode i.e., $\omega_{Rm} < \omega_{CCM} < \omega_{Fm'}$ or $\omega_{Fm'} < \omega_{CCM} < \omega_{Rm}$.

Lasing condition

Case II: $\omega_{Rm} \neq \omega_{Fm'}$, $\Delta\omega \ll \Delta\omega_R, \Delta\omega_F$

Amplitude condition: $$r_A r_B \frac{(\eta e^{g\pi R} - C')^2 + 4C'\eta e^{g\pi R}\sin^2(\delta\beta\pi R)}{(1 - Ce^{g\pi R})^2 + 4Ce^{g\pi R}\sin^2(\delta\beta\pi R)} e^{gL} = 1$$

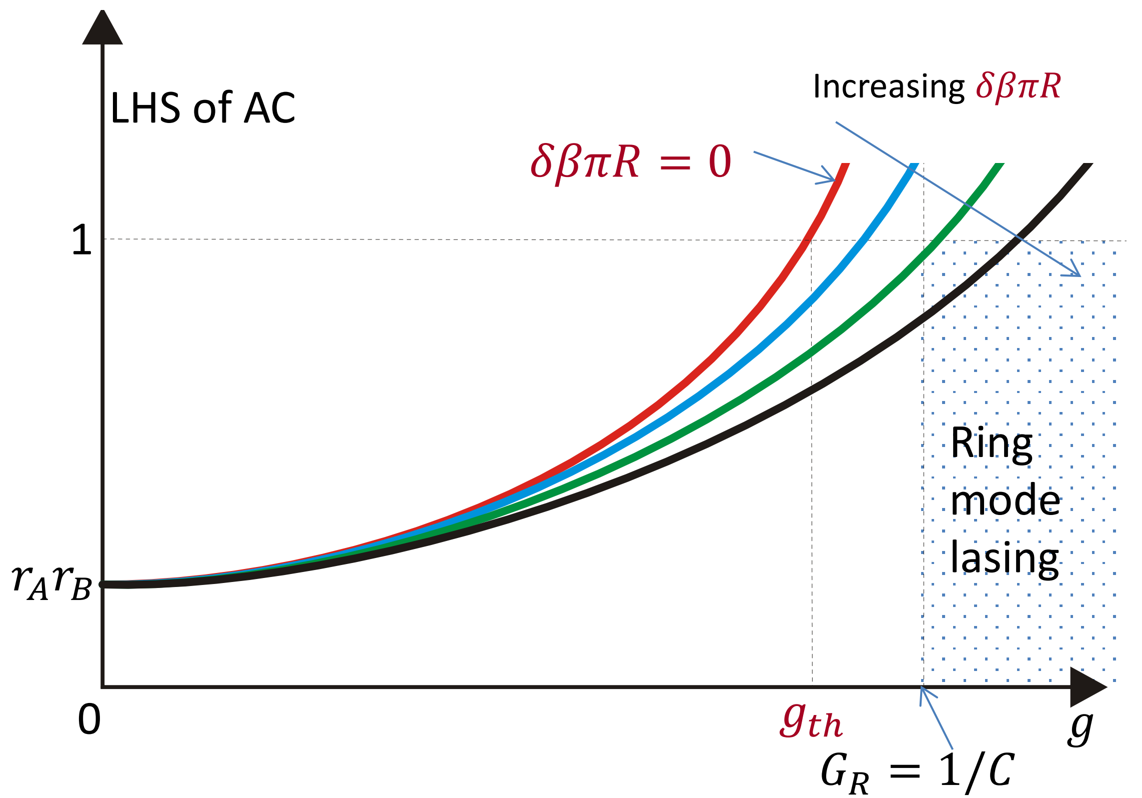

Selection of Lasing Mode

For the case of $2R < L < \pi R$, $\Delta f_F > \Delta f_R$

and common electrode for current injection

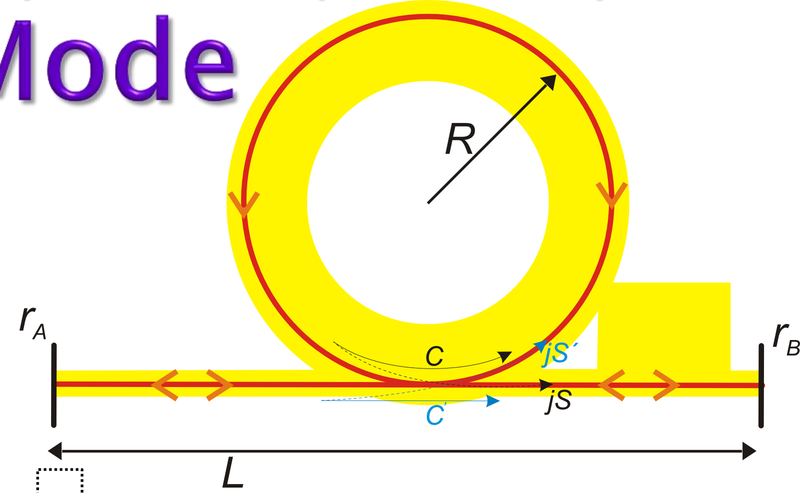

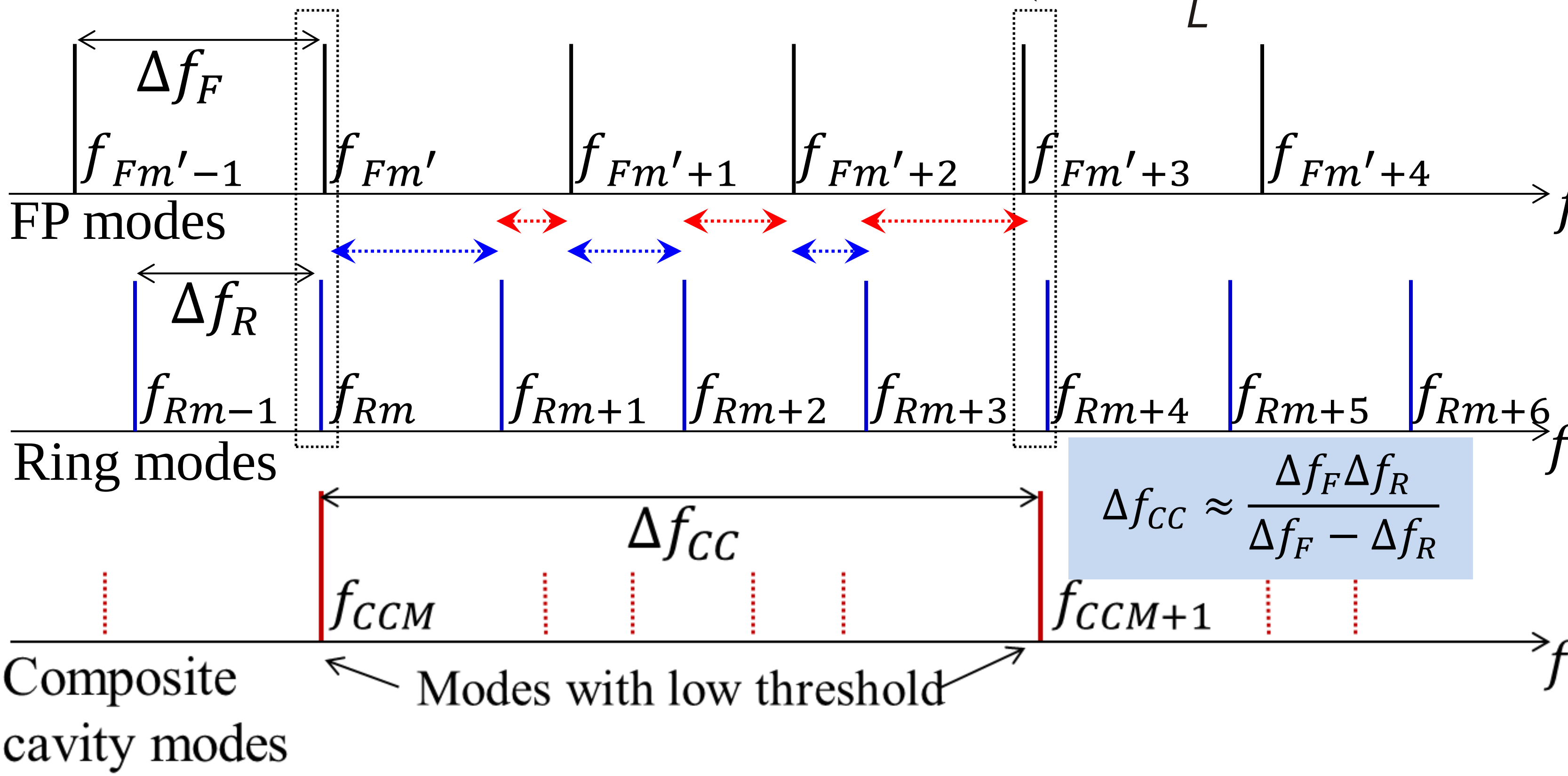

Two-Wavelength Lasing

With separate electrodes for current injection

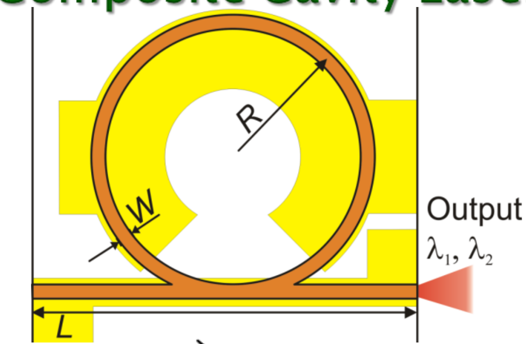

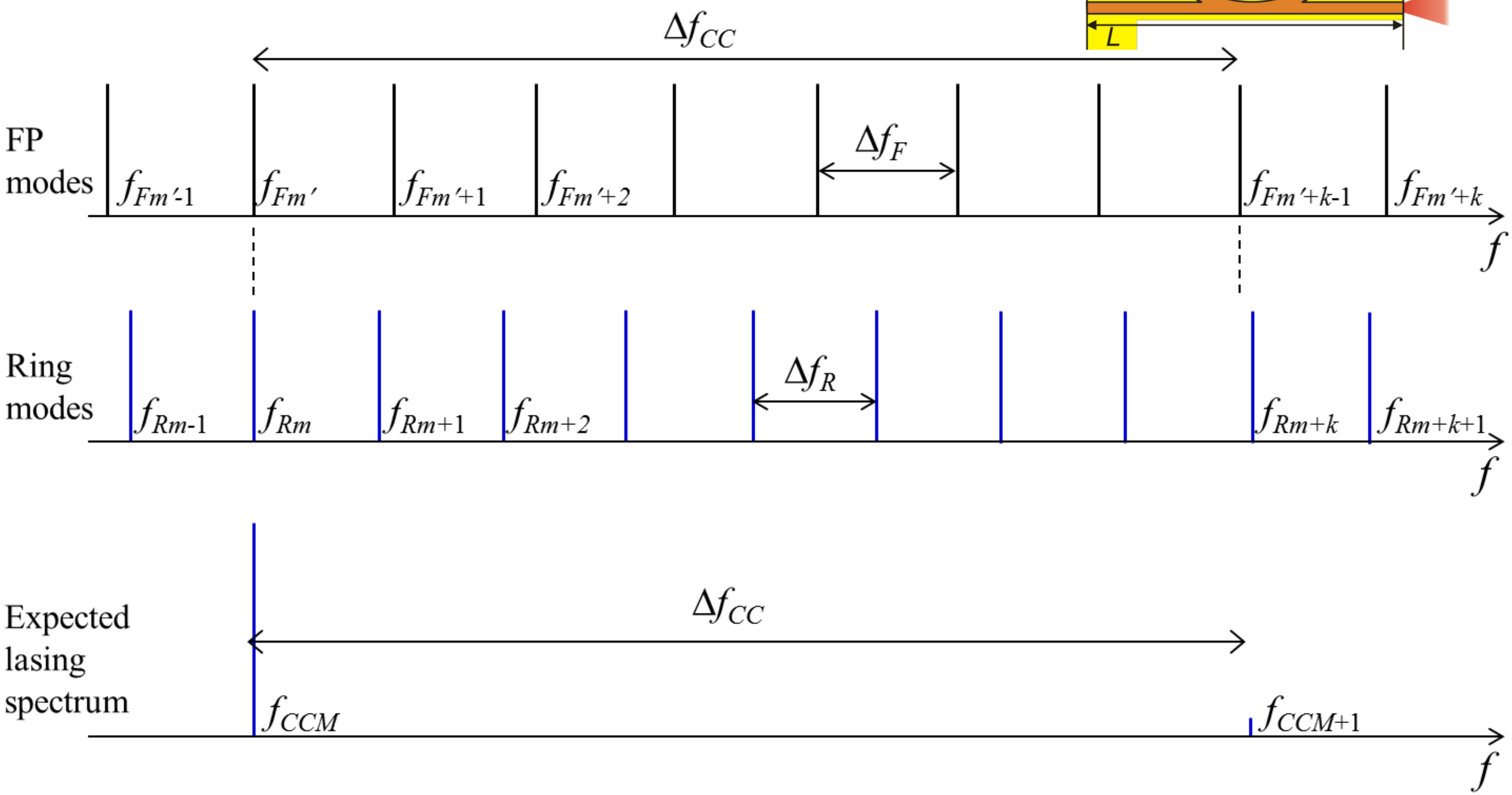

Two-Wavelength Lasing

With separate electrodes for current injection

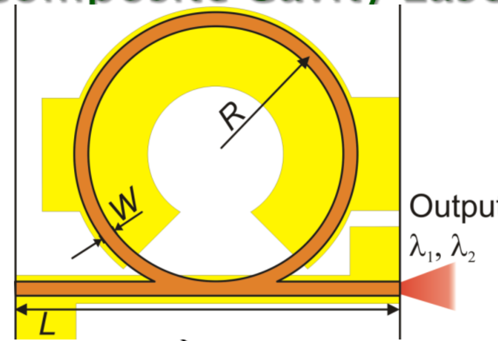

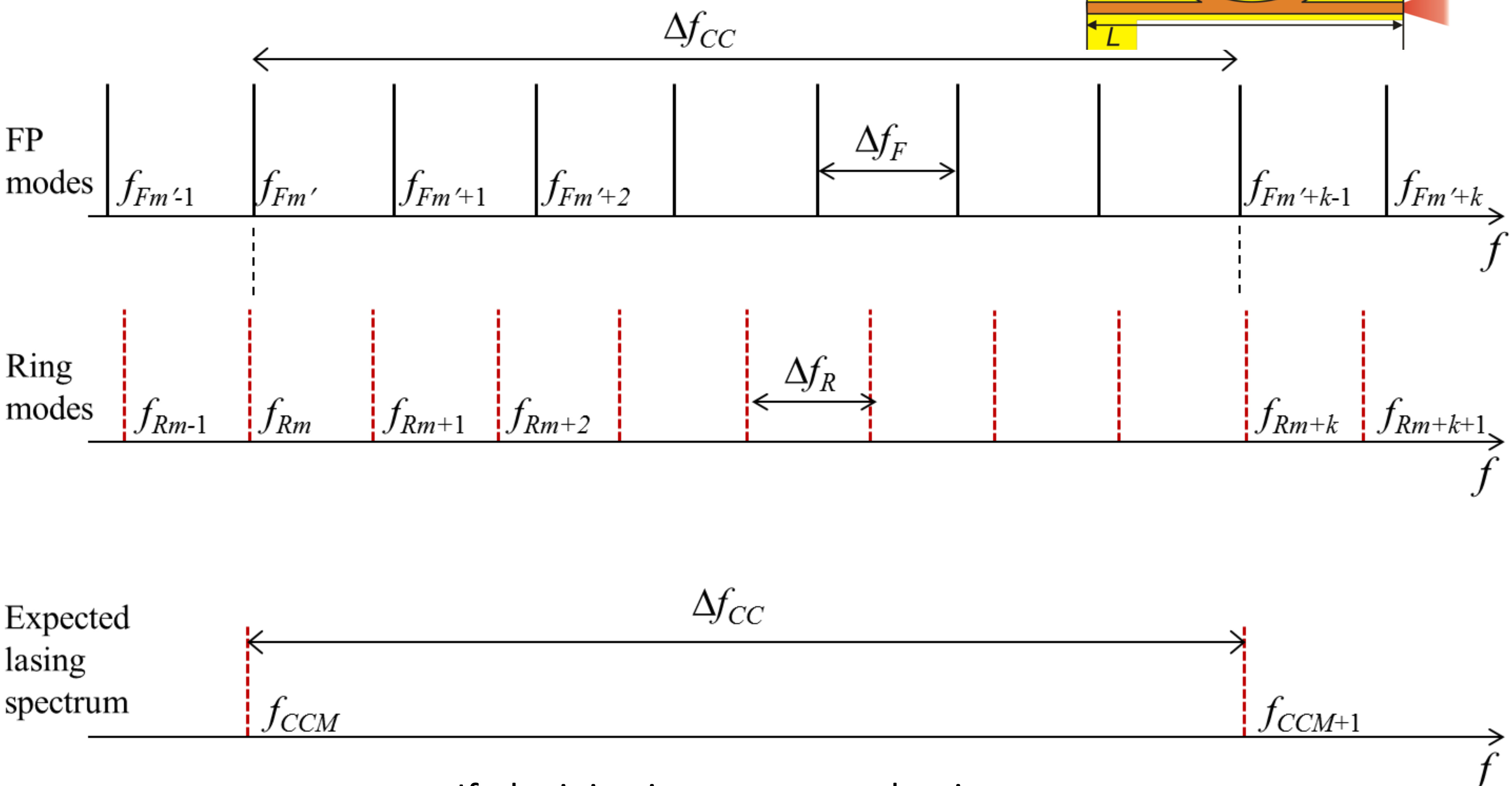

If the injection current to the ring section is increased

Two-Wavelength Lasing

With separate electrodes for current injection

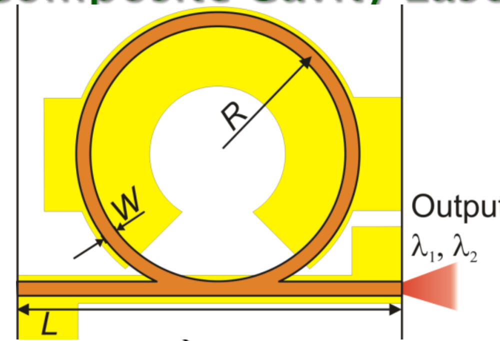

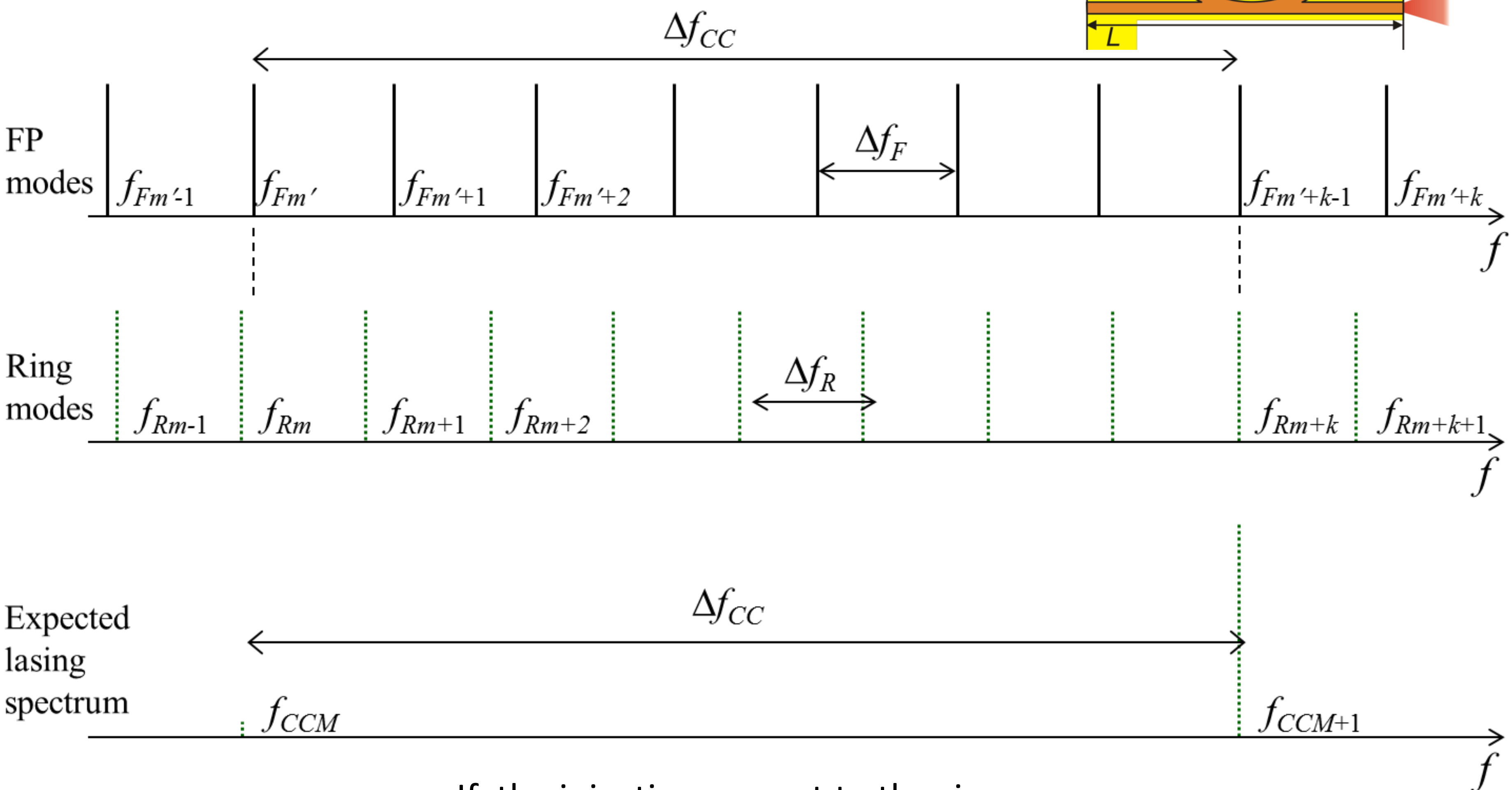

If the injection current to the ring section is increased more

Design of RFP Laser

- $GaAs_{0.86}P_{0.14}$ tensile strained single-quantum-well (SQW) in a separate confinement heterostructure (SCH) with $Ga_{0.51}In_{0.49}P$ guiding layers.
- Using by effective index method, ridge width and height were determined.
- α_b vs R was calculated by the beam propagation method (BPM).
- ***R*=400 μm** was determined, and ***L*=950 μm** was selected as to satisfy $2R<L<\pi R$.

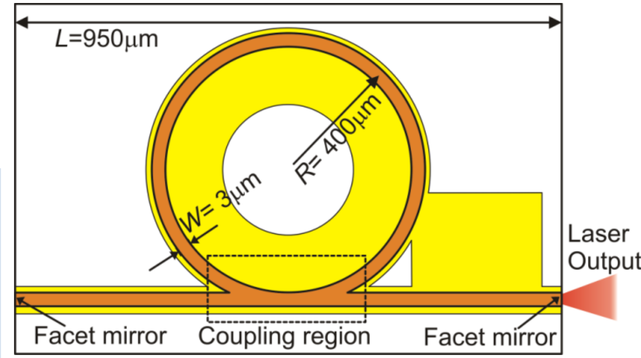

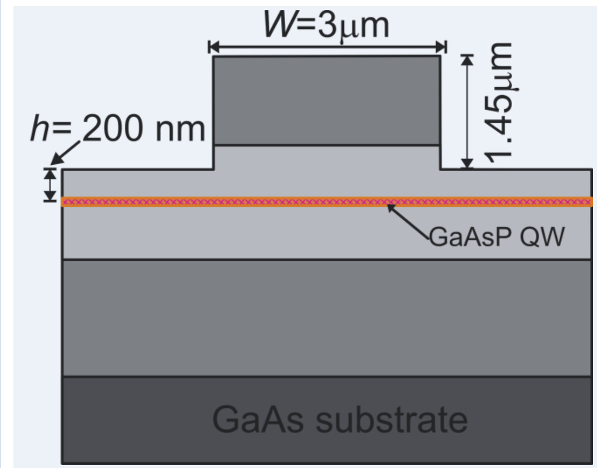

ridge structure

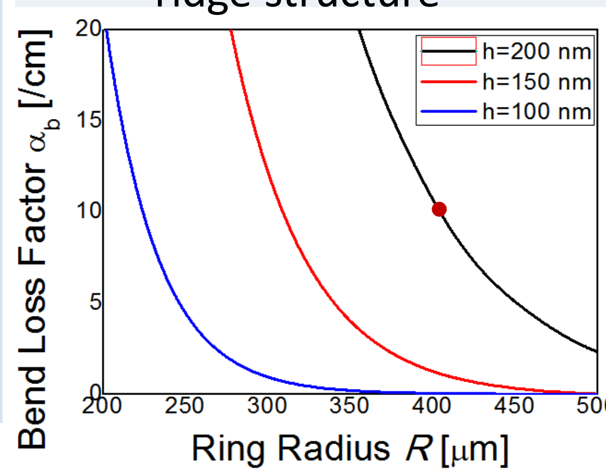

4. Single-Mode RFP Composite Cavity Lasers

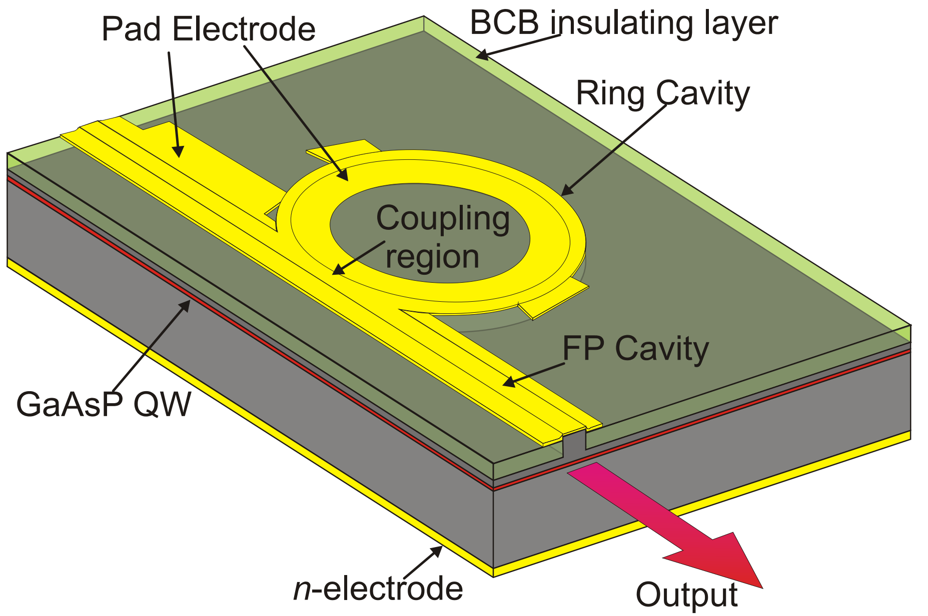

- Novel device structure
- Simple fabrication process
- Stable single mode operation

Fabrication of RFP Laser

The designed RFP laser was fabricated by using a GaAsP SQW epitaxial structure.

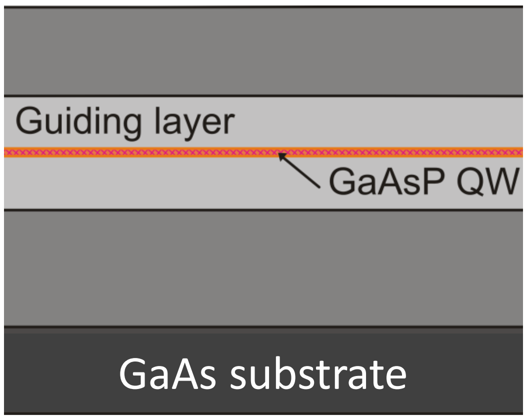

Ridge formation by electron beam (EB) lithography and reactive ion etching (RIE).

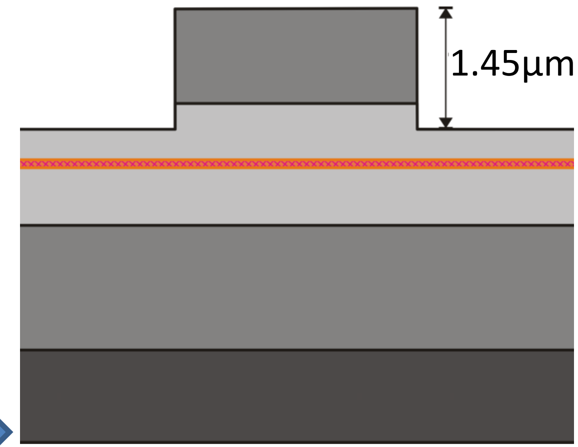

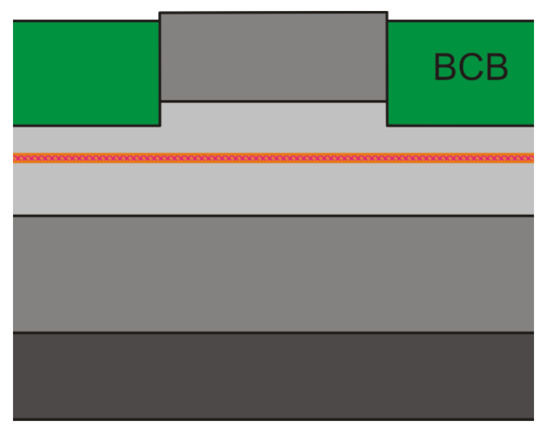

Planarization of entire sample by BCB layer.

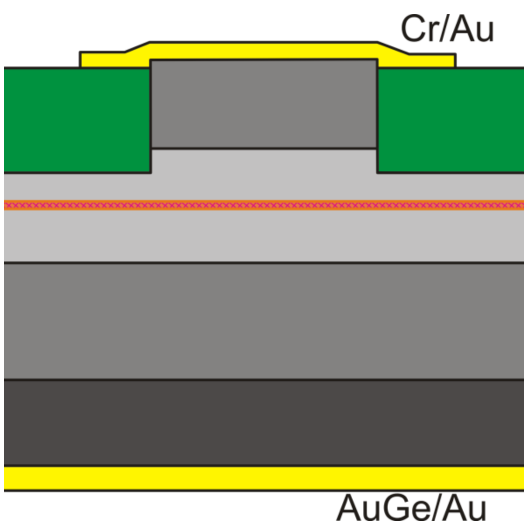

p-side and n-side electrode formation.

Fabricated Single mode RFP Laser

- Fabricated waveguide has smooth and almost vertical side wall.

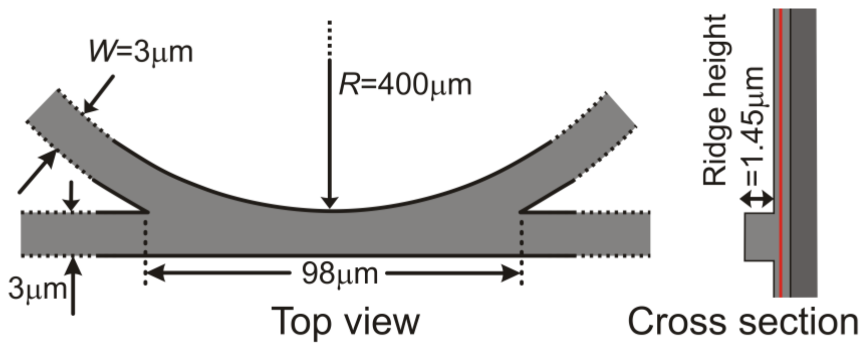

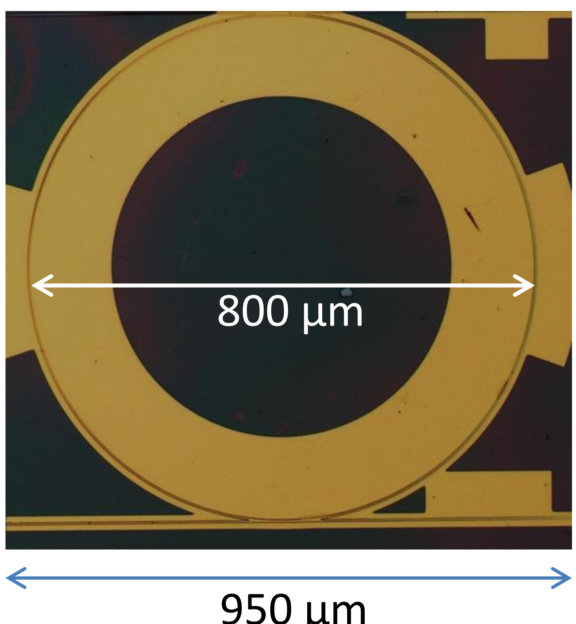

Optical microscopic image

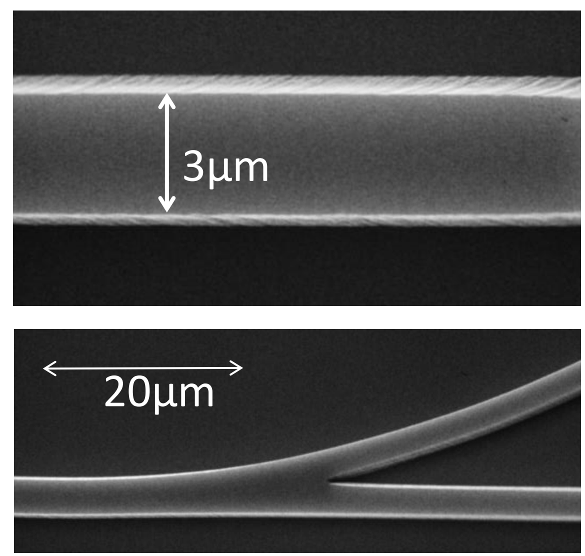

SEM images

Lasing Characteristic

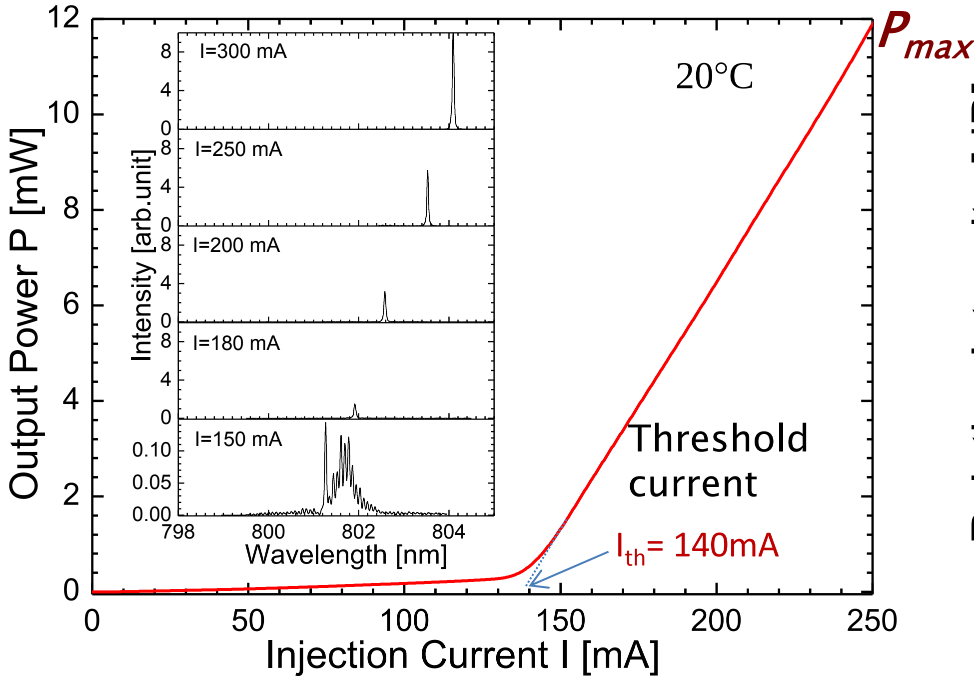

P-I characteristic of the RFP laser

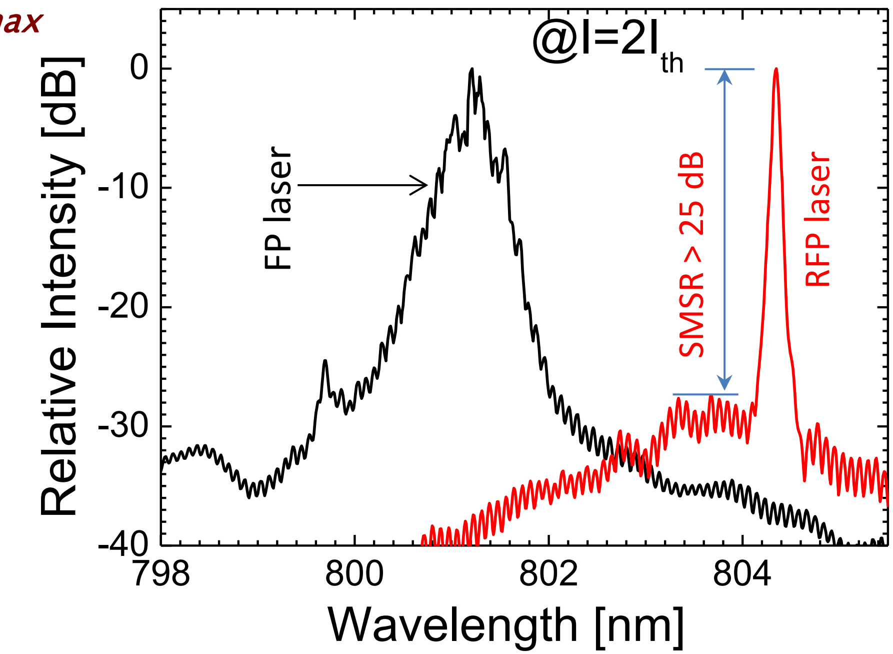

lasing spectra of FP and RFP lasers

- Single mode operation of the RFP laser was achieved with a side mode suppression ratio **(SMSR) greater than 25 dB.**

Temperature Dependence

- Lasing spectra showed the shift of the peak towards longer wavelength region similar to the gain peak shift.

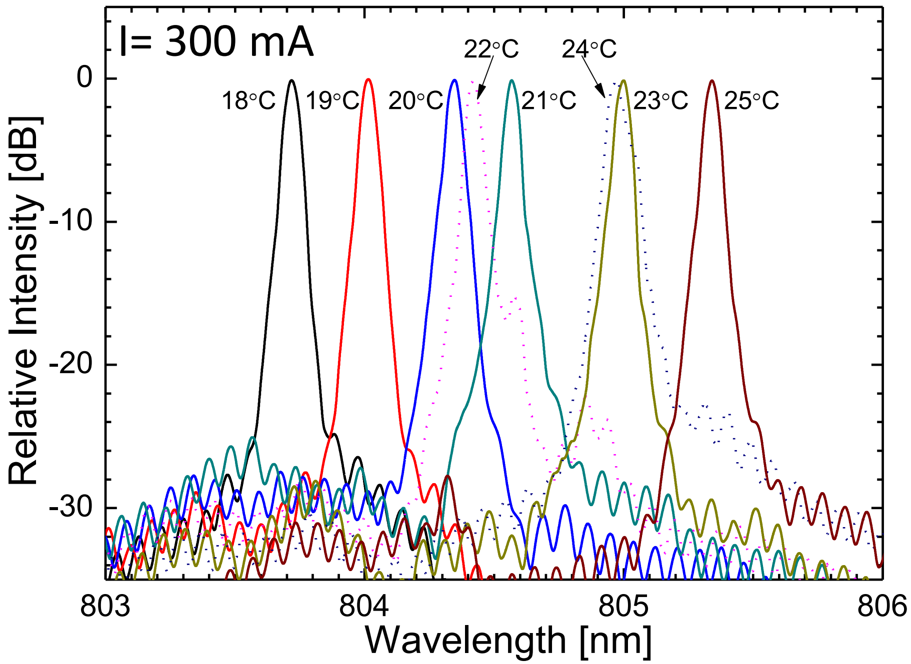

lasing spectra of the RFP laser

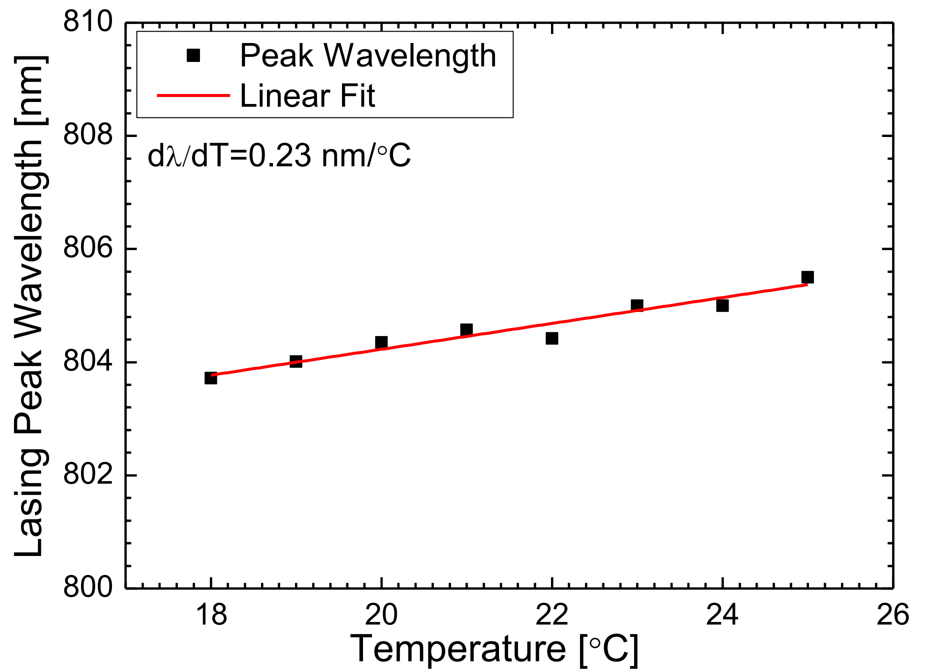

temperature dependence of lasing wavelength

5. Two-Wavelength RFP Composite Cavity Lasers

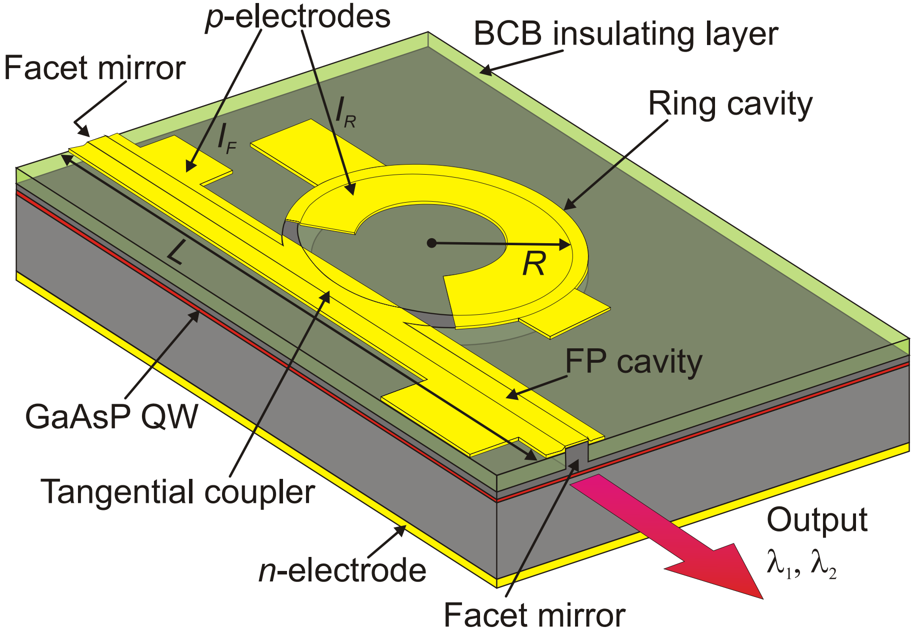

- Simple fabrication process
- Useful for THz wave generation
- Wavelength tunable lasing

RFP Laser with Separate Electrodes

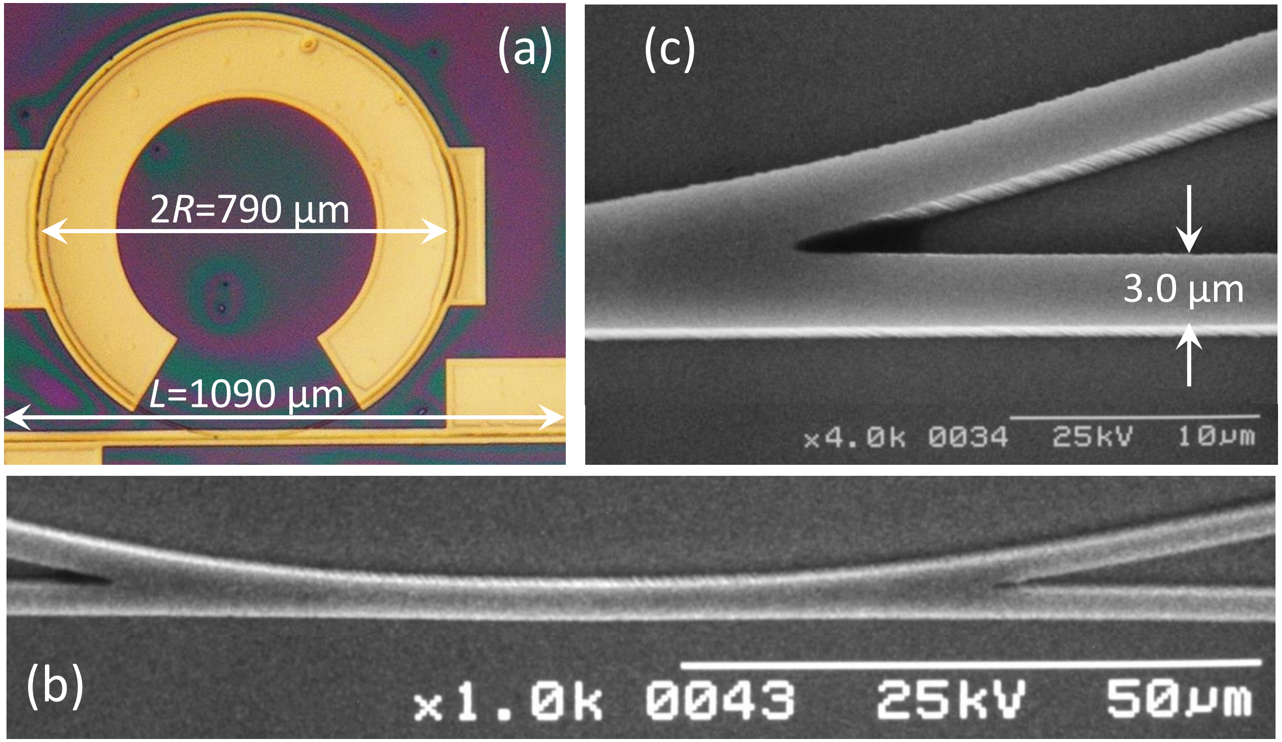

Ridge height
1.55 µm

Optical microscopic and SEM images

Lasing Characteristic

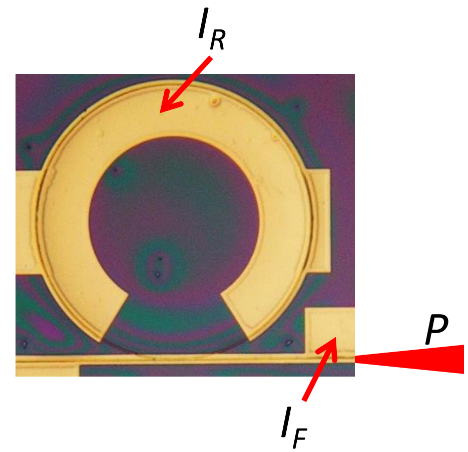

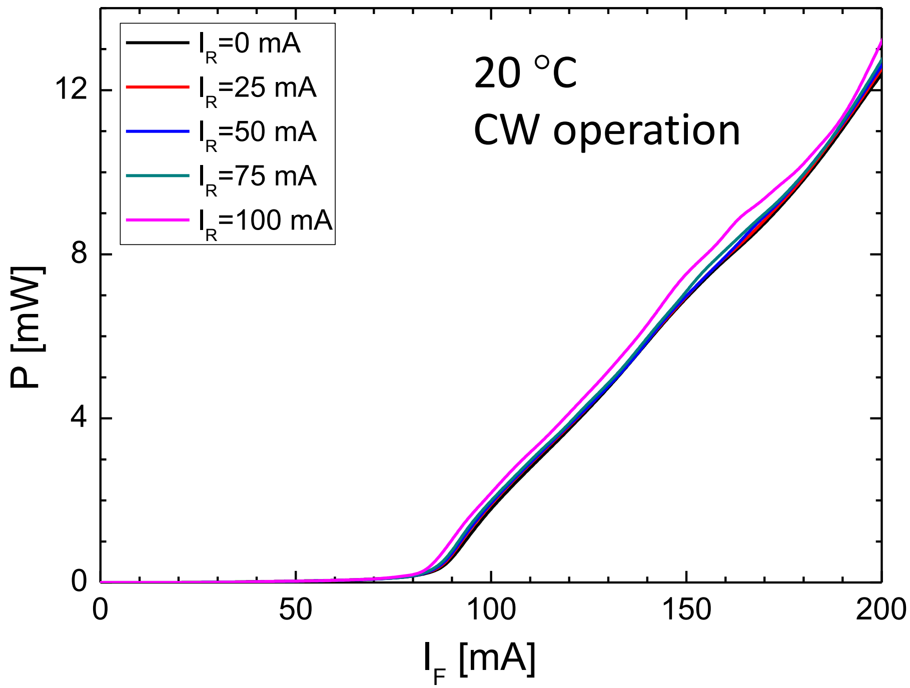

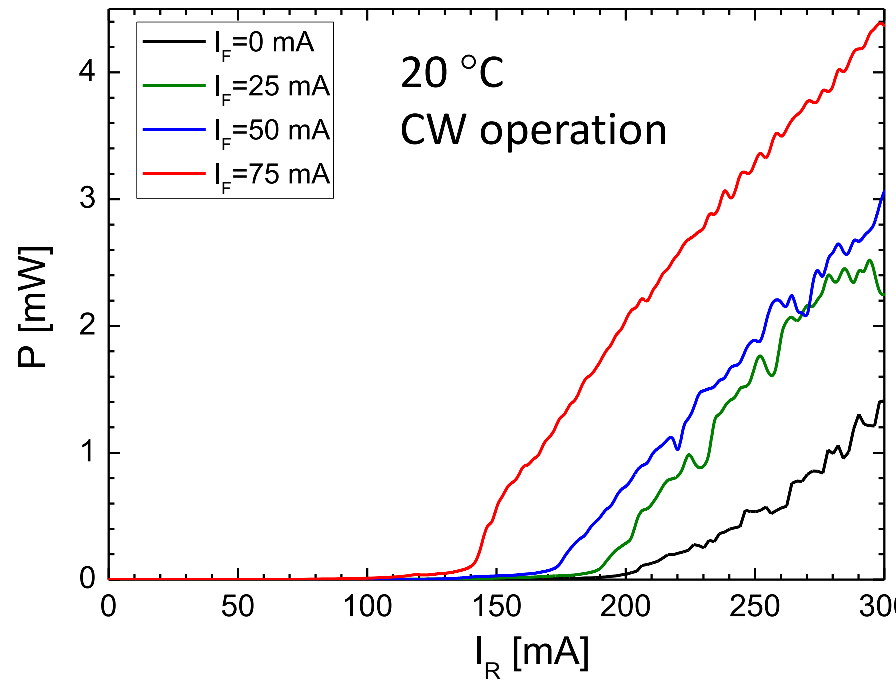

P–I characteristic of the RFP laser

Obtained Two-wavelength Lasing Spectra

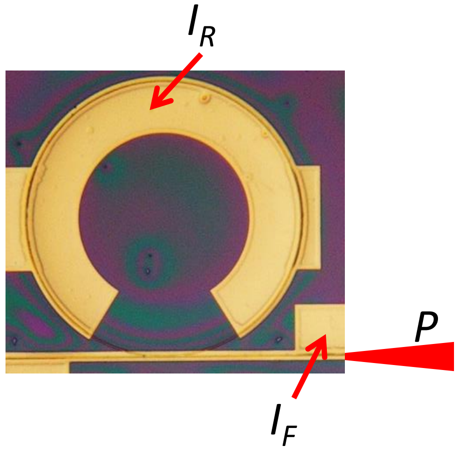

- Currents were injected to both of the ring and straight waveguides.
- I_R was increased slowly and carefully observing the lasing spectrum.
- Accomplished two-wavelength lasing with discrete sets of separations.

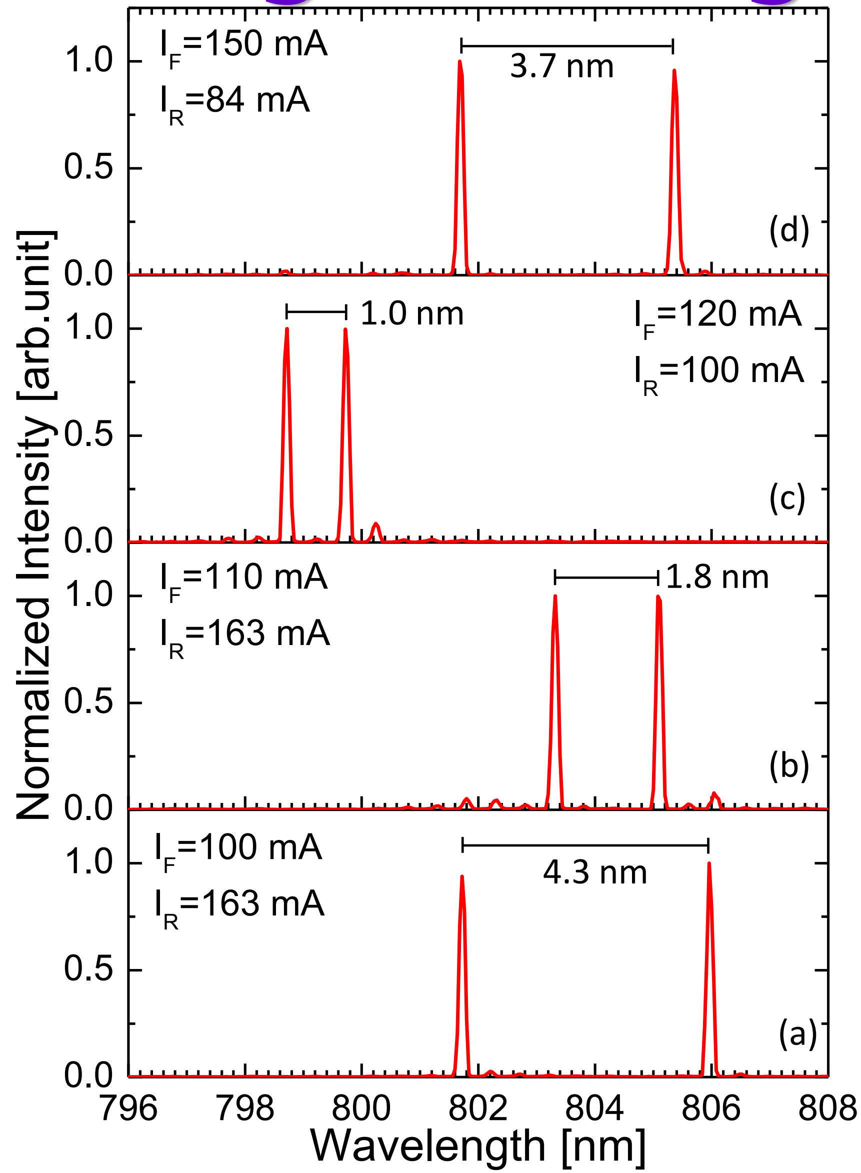

Two-wavelength lasing spectra

Lasing performances

Table I: Summary of driving conditions and obtained two-wavelength lasing performances.

Injection currents I_F, I_R [mA]	Obtained two-wavelength lasing λ_1, λ_2 [nm]	Wavelength separation λ_2-λ_1 [nm]	Total output power [mW]	Power difference [mW]	Beat frequency f_1-f_2 [THz]
100, 163	801.7, 806.0	4.3($\approx 7\Delta\lambda_{CC}$)	3.34	0.11	2.00
110, 163	803.3, 805.1	1.8($\approx 3\Delta\lambda_{CC}$)	4.39	0.0	0.83
120, 100	798.7, 799.7	1.0($\approx 2\Delta\lambda_{CC}$)	4.46	0.0	0.47
150, 84	801.7, 805.4	3.7($\approx 6\Delta\lambda_{CC}$)	7.50	0.16	1.72

For this Laser, $|\Delta\lambda_{CC}|=|(\lambda^2/c)\Delta f_{CC}|\approx 0.59$ nm calculated by using $n_{Reg} = n_{Feg} = 3.624$ for the effective group refractive indices.

6. Conclusions

- **Stitching error free** CGCSEL was fabricated by EB lithography employing smooth circular scanning. Single-mode-like lasing was accomplished and the focusing function was confirmed.
- Idea of a novel all-active **circular ring / FP composite cavity semiconductor laser** was presented. Analysis of lasing threshold and selection of lasing modes were also presented.
- An RFP laser with common p-electrode was fabricated. Stable single longitudinal mode operation was accomplished.
- RFP laser with separate p-electrodes was also fabricated. **Two-wavelength lasing** with discrete sets of separations were accomplished.

- For the first time, I was able to fabricate the stitching error free circular gratings for such a large size device. This unique fabrication technique would further accelerate the research on this type of lasers.
- I also accomplished the two-wavelength lasing with almost equal powers from a single RFP laser for the first time. This device could be a promising candidate for the source of THz wave generation by photomixing process.

List of publications

Journal Papers

[1] **A. K. Saha**, M. Uemukai and T. Suhara, "InGaAs circular-grating-coupled surface emitting laser with focusing function fabricated by electron-beam writing with circular scanning, " Optical Review, vol. 21, no. 3, pp.206-209, June 2014.

[2] **A. K. Saha**, M. Uemukai and T. Suhara, "Single-mode operation of GaAsP ring / Fabry-Perot composite cavity semiconductor lasers," Jpn. J. Appl. Phys., vol. 54, no. 6, 060302, 2015.

[3] **A. K. Saha** and T. Suhara, "Two-wavelength lasing of ring / Fabry-Perot composite cavity semiconductor laser with two separate electrodes," Jpn. J. Appl. Phys., vol. 54, no. 7, 070307, 2015.

Conference Presentations

[1] **A. K. Saha**, T. Sumitani, M. Uemukai and T. Suhara, "Design and Fabrication of InGaAs Quantum Well Circular-Grating-Coupled Surface Emitting Laser," The 60th Japan Society of Applied Physics (JSAP) Spring Meeting, 29a-B4-9 (2013-03).

[2] **A. K. Saha**, T. Sumitani, M. Uemukai and T. Suhara, "Lasing Characteristic of InGaAs Circular-Grating-Coupled Surface Emitting Laser with Focusing Function," The 61th Japan Society of Applied Physics (JSAP) Spring Meeting, 18p-F9-13 (2014-03).

[3] **A. K. Saha**, M. Uemukai and T. Suhara, "Single-Mode Operation of GaAsP Ring/Fabry-Perot Composite Cavity Semiconductor Lasers," Institute of Electronics, Information and Communication Engineers (IEICE) Technical Report, vol. 114, no. 432, LQE2014-176, pp. 237-240, (2015-01).

[4] **A. K. Saha** and T. Suhara, "Demonstration of Two-Wavelength Lasing in a GaAsP Ring/Fabry-Perot Composite Cavity Semiconductor Laser", *submitted for presentation in* 2015 International Conference on Solid State Devices and Materials (SSDM 2015), (Sapporo, Hokkaido, Japan).

Thank you very much
for your kind
attention.